

## Durham Research Online

---

### Deposited in DRO:

18 June 2020

### Version of attached file:

Accepted Version

### Peer-review status of attached file:

Peer-reviewed

### Citation for published item:

Lúcio, Thales and Souza Neto, João Adauto and Selby, David (2020) 'Late Barremian / Early Aptian Re-Os age of the Ipubi Formation black shales : stratigraphic and paleoenvironmental implications for Araripe Basin, northeastern Brazil.', *Journal of South American earth sciences.*, 102 . p. 102699.

### Further information on publisher's website:

<https://doi.org/10.1016/j.jsames.2020.102699>

### Publisher's copyright statement:

© 2020 This manuscript version is made available under the CC-BY-NC-ND 4.0 license  
<http://creativecommons.org/licenses/by-nc-nd/4.0/>

### Additional information:

---

### Use policy

The full-text may be used and/or reproduced, and given to third parties in any format or medium, without prior permission or charge, for personal research or study, educational, or not-for-profit purposes provided that:

- a full bibliographic reference is made to the original source
- a [link](#) is made to the metadata record in DRO
- the full-text is not changed in any way

The full-text must not be sold in any format or medium without the formal permission of the copyright holders.

Please consult the [full DRO policy](#) for further details.

**Late Barremian / Early Aptian Re-Os age of the Ipubi Formation black shales: stratigraphic and paleoenvironmental implications for Araripe Basin, Northeastern Brazil**

Thales Lúcio<sup>a,\*</sup>, João Adauto Souza Neto<sup>a</sup>, David Selby<sup>b,c</sup>

<sup>a</sup> Geochemistry Laboratory Applied to Petroleum, Department of Geology, Graduate Program in Geosciences, Federal University of Pernambuco, Recife 50.740-550, Brazil  
<thales.lucio@ufpe.br, adauto@ufpe.br>

<sup>b</sup> Department of Earth Sciences, Durham University, Durham, DH13LE, UK

<sup>c</sup> State Key Laboratory of Geological Processes and Mineral Resources, School of Earth Resources, China University of Geosciences, Wuhan, 430074, Hubei, China

\* Corresponding author. Address: Universidade Federal de Pernambuco, Centro de Tecnologia e Geociências, Departamento de Geologia, Av. da Arquitetura, s/n, Cidade Universitária, 50740-550, Recife, PE, Brasil, Tel: +55 81 997220853

**Abstract**

The Ipubi Formation of the Santana Group, Araripe Basin, Brazil, is characterized by black shales and overlying evaporite deposits and is suggested to record the transition from lacustrine to marine depositional environments. To date, the age of the black shales, constrained only by microfossils, is poorly determined, with ages spanning ~25 myrs from 125 to 100.5 Ma (Aptian-Albian). Here we present new Re-Os elemental and isotopic data to provide the first absolute age for those rocks of the Ipubi Formation and an improved understanding of the depositional paleoenvironment of the Araripe Basin. The Re-Os isotope data for Ipubi Formation black shales yields a depositional age of  $123 \pm 3.5$  Ma, with a highly radiogenic initial  $^{187}\text{Os}/^{188}\text{Os}$  composition ( $\text{Os}_i$ ) of  $1.97 \pm 0.02$ . The Re-Os age indicates that the deposition of the Ipubi Formation black shales occurred during the Late Barremian / Early Aptian, prior to the onset of OAE 1a, in a highly restricted marine / lacustrine setting.

**Keywords**

Geochronology; Rhenium-Osmium; Barremian / Aptian boundary; Restricted marine

## 1. Introduction

Located in northeastern Brazil, the Araripe Basin, in the Borborema Province, is characterized by a Pre-Cambrian basement that exhibits a predominant northeast-southwest structural orientation. As a result, the architecture of the Araripe Basin is strongly characterized by horsts and grabens, that were formed in association with the rifting of Gondwana and the opening of the South Atlantic during the earliest Cretaceous (Hauterivian; Fig. 1; Matos, 1992; Ponte and Ponte Filho, 1996). The Araripe Basin comprises the Vale do Cariri, and the Chapada do Araripe regions that exhibit positive, tabular, and elongated E-W relief with sedimentary strata that gently dip to the west (Assine, 2007). Deposited into an intracratonic setting, the Paleozoic Cariri Formation represents the earliest sedimentation in the basin (Assine, 2007). Mesozoic successions comprise the pre-rift Cretaceous Neocomian Brejo Santo and Missão Velha formations, syn-rift Berriasian-Hauterivian Abaiara Formation, post-rift I Aptian-Albian Santana Group (Barbalha, Crato, Ipubi and Romualdo formations), and the post-rift II Albian-Cenomanian Araripe Group (Arapipina and Exu formations; Fig. 2; Ponte and Ponte Filho, 1996; Batten, 2007; Assine, 2007; Scherer et al., 2014; Assine et al., 2014; Neumann and Assine, 2015; Fambrini et al., 2019).

The Araripe Basin has received significant attention, mainly because of its rich fossil content of the Santana Group (Crato and Romualdo formations) which have been utilized for paleoenvironmental, paleoclimatic, paleoecologic and paleogeographic reconstructions (Beurlen, 1964; Lima, 1978; Arai, 2012, 2014; Tomé et al., 2014; Sucerquia et al., 2015; Prado et al., 2015; Pereira et al., 2016; Field and Martill, 2017; Oliveira and Kellner, 2017). The Crato Formation includes one of the most critical terrestrial arthropod assemblages in the world due to the presence of primitive mayfly, dragonfly, earwig, grasshoppers, beetles, butterflies, spiders and scorpions (Martill et al., 2007). Ostracods, conchostracans and a rare caridean shrimp represent the crustaceans (Schweigert et al., 2007). Fossilized fish are dominated by *Dastilbe crandalli*, *Cladocycilus*, *Lepidotes* and *Araripelepidotes* (Davis and Martill, 1999), with *Vinctifer*, *Cladocycilus*, *Rhacolepis*, *Notelops*, *Mawsonia* and *Axelrodichthys* also being present in the Romualdo Formation. Further, well preserved wing membranes and wing fibres, claw sheaths, foot webs, and a heel pad of pterosaurs (*Arthurdactylus*, *Ludodactylus*, *Ingridia*, *Santanadactylus*, *Araripesaurus*, *Cearadactylus*, *Brasileodactylus*, *Anhanguera*, *Lacusovagus*) have been discovered from the Crato and

Romualdo formations (Martill and Unwin, 1989; Martill and Frey, 1998; Frey et al., 2003; Unwin and Martill, 2007; Witton, 2007), with additional dinosaurs (*Irritator*, *Angaturama*, *Santanaraptor* and *Mirischia*) being known in the Romualdo Formation (Kellner, 1996, 1999; Martill et al., 1996, 2000).

The age attributed to the whole ~~entire~~ Santana Group is indicated ~~characterized~~ by the *Cytheridea* spp. 201-208 Zone (NRT-011; Fig. 3; Coimbra et al., 2002). In contrast, ~~the~~ ~~diverse~~ palynomorphs reported to this group define two palynozones: the *Sergipea variverrucata* Zone (Barbalha and Crato formations) and the *Cicatricosisporites avnimelechi* Zone (Ipubi and Romualdo formations; Coimbra et al., 2002). These zones coincide with the interval between the Rio da Serra and Alagoas local stages (Berriasian to Aptian). Nevertheless, microfossils (e.g. *Pattersonocypris angulata*, *Pattersonocypris micropapillosa*, *Alicenula leguminella*) present in the Santana Group suggest that the Ipubi and Romualdo formations were deposited during the temporal framework of the Aptian and Albian stages (Regali, 1990; Coimbra et al., 2002). The presence of *Darwinula* in the ~~argillite~~ greenish mudstone that ~~infill~~ occurring filling fractures ~~in~~ crosscutting the evaporites overlying the black shales (both lithologies of the Ipubi Formation) and the presence of a single gyrogonite of Charophyta, has resulted in a *Darwinula*-Charophyta association for the Crato, Ipubi and Romualdo formations. Thus, this is considered to ~~which~~ constrain the age of the Ipubi Formation black shales to the Aptian and Albian stages (Fig. 3; Silva, 1975; Silva-Telles and Vianna, 1990; Neumann, 1999; Tomé et al., 2014).

Therefore, ~~our current knowledge of~~ until now the age ~~and evolution~~ of the Ipubi Formation is based solely on biostratigraphy, which constrains the deposition of the Ipubi Formation to a ~25 myr interval ~~that encompasses both~~ within the Aptian and Albian. To provide an improved understanding of the deposition timing of the Ipubi Formation and the entire Santana Group, and the evolution of the Araripe Basin, here we apply the rhenium-osmium isotope chronometer to the Ipubi Formation black shales and in turn show that the formation can be tied to the latest Barremian / earliest Aptian that was deposited in a lacustrine/highly restricted marine-influenced paleo-setting.

## 2. Geological aspects of the Ipubi Formation

The Ipubi Formation stratigraphically lies between the lacustrine limestones of the underlying Crato Formation and the marine calciferous sandstones and mudstones of the



overlying Romualdo Formation (Ponte and Appi, 1990; Assine, 1992, 2007; Neumann and Cabrera, 1999; Assine et al., 2014; Neumann and Assine, 2015). Previous research has proposed that the post-rift phase I interval is represented by the Santana Formation, with the Crato, Ipubi and Romualdo being members, or even named differently (e.g., Santana Formation instead Romualdo Formation; Beurlen, 1971; Lima, 1979; Assine, 1994; 2007; Martill, 2007). More recently, it has been suggested that the Ipubi black shales and evaporites is a unit within the Crato Member (limestones) of the Santana Formation, with the different lithologies recording lateral variations that were deposited contemporaneously based on the order of marine evaporites and the absence of subaerial exposure and erosion (e.g., Bobco et al., 2017; Goldberg et al., 2019). However, regional lithology interdigitation of the Crato Formation with the Ipubi Formation evaporite is not observed (Bobco et al., 2017; Goldberg et al., 2019). Further, the proposal of interdigitation does not consider the presence of regionally recognized subaerial exposure that separates the Crato, Ipubi, and Romualdo units (Silva, 1986; Neumann and Cabrera, 1999; Assine et al., 2014; Neumann and Assine, 2015; Fabin et al., 2017). For example, the top of the Crato Formation is composed of calcrete formed under subaerial conditions (Neumann and Cabrera, 1999; Fabin et al., 2017), and the top of Ipubi Formation that is characterized by a subaerial exposure and erosion (karst surface) marked by large isolated columns and scattered depressions, pits and escarpments composed by clasts of gypsum, shale, fine-to-medium sandstone and quartz pebbles (Silva, 1986; Fabin et al., 2017). Lastly, based on mapping, stratigraphical correlation and sequence stratigraphy (well-known criteria considered to establish lithostratigraphic units according to Stratigraphic Guide by International Commission on Stratigraphy), the stratigraphic status of Ipubi and Santana units were changed to “Formation” and “Group”, respectively (Neumann and Cabrera, 1999; Neumann and Assine, 2015). Based on the latter and our observation in both outcrop and boreholes we adopt the stratigraphic proposal of Neumann and Assine (2015).

In the post-rift phase I tectonic-sedimentary sequence of Araripe Basin, the Ipubi Formation comprises an evaporite (gypsum and anhydrite) interval 12-30 m thick associated with black shales of up to 5 m thick from its base, totaling 30 to 40 m in thickness (Neumann and Assine, 2015; Fabin et al., 2017). In the southwestern border region of the Araripe Basin, this formation directly overlies the Precambrian basement units (3.4 to 2.1 Ga; Silva et al., 1997; Fetter et al., 1999; Sato et al., 2012; Ancelmi,

2016; Martins, 2017; Vale, 2018). In contrast, in the northeastern region of the basin the Ipubi Formation overlies limestone of the Crato Formation or units of older (Early Cretaceous) tectonic-sedimentary phases of the basin (Neumann and Cabrera, 1999; Assine et al., 2014; Fabin et al., 2017). Concerning the representative area chose to sampling in this contribution, in the southwestern part of the basin, the Ipubi Formation black shales are characterized by dark to gray shales, mudstones, and carbonates, laminated, ostracode-rich, with pyrite and are bituminous (this study; Assine et al., 2014; Goldberg et al., 2019). Regionally, the upper portion of the black shale interval is interbedded with the gypsum lenses (< 10 cm wide) and bedding-parallel fibrous gypsum veins (Fabin et al., 2017). In the middle of the evaporite sequence, a sub-horizontal unconformity can regionally be observed in both the southwestern and northeastern borders of the basin (Souza Neto et al., 2013), which is filled by succession (40-60 cm wide) composed, from bottom to top, by plant fossil-bearing greenish mudstones, ostracod-conchostracan-rich laminated marls and thin black shales, and with gypsum-lenses (Souza Neto et al., 2013; Assine et al., 2014; Goldberg et al., 2019). Detailed petrographic observations and XRD analyses indicate that the black shales are predominantly composed of clay minerals (essentially illite-smectite), calcite, K-feldspar, quartz and minor celestite, apatite, and sulfides (Souza Neto et al., 2013; Nascimento Jr et al., 2016). The rocks are organic matter rich (TOC > 10 to 29 %; Souza et al., 2013; Castro et al., 2017), with both liquid chromatography data ((saturated + aromatic)/(polar) hydrocarbon ratios from 0.12 to 0.88; Lúcio et al., 2016a) and pyrolysis data indicating the shales to be hydrocarbon immature ( $T_{max} < 435^{\circ} \text{C}$  and  $PI < 0.1$ ; Castro et al., 2017) but endowed with a large gas potential ( $S_2 < 200 \text{ mg/g}$ ; Castro et al., 2017). Pristane/Phytane ratios of < 1 (Silva et al., 2014; Castro et al., 2017) and  $V/(V + Ni)$  ratios between 0.6 and 0.8 (Lúcio et al., 2016b) of the shales propose deposition under reducing conditions.

The presence of dinoflagellates (*Spinierites* and *Subtilisphaera*; Arai and Coimbra, 1990) and palynoforaminifers (organic linings and allied material; Lima, 1978; Arai, 2012; Goldberg et al., 2019), predominance of odd-to-even *n*-alkanes (Silva et al., 2014), and low organic phosphorus content (< 2 %; Souza Neto et al., 2013) in the black shales is interpreted to indicate deposition in a marine setting, which is supported by the sulphur isotope data ( $\delta^{34}\text{S} = \sim 10$  to 18 ‰; Bobco et al., 2017) of the overlying evaporite unit. However, a pure marine setting for Ipubi Formation black shales is not supported

by the presence of non-marine ostracods (*Harbinia alta* and *Darwinula*; Antonietto et al., 2012; Tomé et al., 2014) and lacustrine facies (Assine, 2007; Assine et al., 2014). Based on the presence of evaporites, the Southern Australian sabkha environment has been proposed as a modern day analogue model for the paleogeography of the Ipubi Formation (Silva, 1988; Oliveira et al., 1979; Assine, 2007; Assine et al., 2014; Bobco et al., 2017; Fabin et al., 2017; Goldberg et al., 2019). being known as a shoreline with a restricted connection to the open ocean (Warren, 2016).

### 3. Sampling and analytical methods

Nine samples of black shales were collected from the Ipubi Formation in the southwestern portion of the Araripe Basin from the open pit Campevi mine in Gergelim County that excavates the evaporate of the Ipubi Formation (Fig. 2). The Ipubi Formation black shales occur stratigraphically below the evaporite sequence and are present beneath the quarry floor. To sample the formation, trenches in the quarry floor were dug about 1 m vertically beneath the surface exposure and ~4 m laterally from each other. The trenches were dug to expose a 1 m stratigraphic interval of the Ipubi Formation black shales (Fig. 4). All exposed surfaces showed black shales with variations in their facies (described below), were unweathered and care was taken to avoid zones of fractures and gypsum-veins and -lenses that were present in some trenches. The stratigraphic profile (Fig. 4) of the black shale unit comprises from bottom to top a 20 cm thick bituminous mudstone with an incipient laminar structure (~20 cm wide) that is overlain by a 30 cm interval of bituminous black shale exhibiting a millimeter to centimeter intercalated succession of light-coloured marls. The latter is overlain by 50 cm interval of bituminous laminated black shale that is fossiliferous (plants, preferentially preserved with a brown and phosphate-rich coating), with pyrite-bearing nodules (< 5 mm diameter), and gypsum-rich lenses (> 3 cm long). Samples were collected at a same deep position, about 1 m, predominantly from the mudstone and black shale interbedded marl horizons (see Table 1 for detail).

At the Laboratory of Geochemistry Applied to Petroleum at the Federal University of Pernambuco, the samples were washed with deionized water, then dried (at 60 °C for ~12 h) in an oven and powdered (~25 g) in an electric agate grinder (Pulverisette 7 classic line). The organic matter (OM %) and carbonate contents (CaCO<sub>3</sub> %) were obtained by weight-loss (at 360 °C for ~4 h and 1050 °C for ~1 h, respectively) and

aluminium content (Al ppm) by Energy Dispersive X-ray Fluorescence (EDXRF), respectively (Table 1). The Al content was used to calculate the enrichment factor of both Re and  $^{192}\text{Os}$  content in the organic-rich sampled horizon (Algeo and Maynard, 2004; Tribovillard et al., 2006; Table 1).

The Re and Os isotopic compositions and elemental abundances for the rock powders were determined at the Durham Geochemistry Center at Durham University. Approximately ~1 g of sample powder was digested with a mixed tracer (spike) solution of  $^{190}\text{Os}$  and  $^{185}\text{Re}$  in a  $\text{Cr}^{\text{VI}}\text{-H}_2\text{SO}_4$  solution at 240 °C for ~48 h (cf. Selby and Creaser, 2003). The  $\text{Cr}^{\text{VI}}\text{-H}_2\text{SO}_4$  dissolution media selectively liberates the hydrogenous Re and Os from the sediment limiting any detrital contribution (Selby and Creaser, 2003; Kendall et al., 2004). Rhenium and osmium were purified from the acid solution using solvent extraction, micro-distillation and anion chromatography methods. The purified Re and Os fractions were loaded onto Ni and Pt filaments, respectively (Selby et al., 2007), with the isotopic measurements conducted using negative thermal ionization mass spectrometry (Creaser et al., 1991) on a Thermo Scientific TRITON mass spectrometer via static Faraday collection for Re and ion-counting using a secondary electron multiplier in peak-hopping mode for Os in the Arthur Holmes Laboratory at Durham University.

The uncertainties for  $^{187}\text{Re}/^{188}\text{Os}$  and  $^{187}\text{Os}/^{188}\text{Os}$  was performed by error propagation incorporating uncertainties from the Re and Os mass spectrometer measurements, total blank abundances (Re =  $12 \pm 1$  pg, Os =  $0.08 \pm 0.02$  pg) and Os isotopic composition ( $^{187}\text{Os}/^{188}\text{Os} = 0.23 \pm 0.01$ ), spike calibrations, and reproducibility of standard Re and Os isotopic values. The Re-Os isotopic data,  $2\sigma$  calculated uncertainties for  $^{187}\text{Re}/^{188}\text{Os}$  and  $^{187}\text{Os}/^{188}\text{Os}$  and the associated error correlation function ( $\rho$ ; Ludwig, 1980) are regressed using the beta version of Isochron program (Li et al., 2019) which incorporates the benchmark Isoplot algorithm (Ludwig, 2012) and the Monte Carlo sampling method for error propagation to yield a Re-Os age using the  $\lambda^{187}\text{Re}$  constant of  $1.666\text{e}^{-11} \pm 5.165\text{e}^{-14} \text{ a}^{-1}$  (Smoliar et al., 1996).

In the beta version of Monte Carlo Isochron technique (Li et al., 2019), a prescribed number of isochrons ( $10^6$ ) are created from the input data and their corresponding probability density function (analytical uncertainty of  $^{187}\text{Re}/^{188}\text{Os}$  and  $^{187}\text{Os}/^{188}\text{Os}$  values, and their error correlation,  $\rho$ ). The age and  $\text{Os}_i$  estimate for each iteration are

crossed plotted yielding a probabilistic distribution that includes analytical uncertainty. Model uncertainties, those attributed to the isochron linear regression, are also calculated. In the Isoplot program (Ludwig, 2012), a Model 1 age implies that the assigned  $2\sigma$  uncertainties and calculated error correlations are the only cause of the scatter in the data-points from the regression line; whereas a Model 2 best-fit assigns equal weight and zero error-correlations to each point; in contrast, a Model 3 age assumes that the scatter about the isochron line may be linked to both geological factors that produce variation in the initial  $^{187}\text{Os}/^{188}\text{Os}$  values and the assigned analytical uncertainties. The isoplot program also yields the Mean Square of Weighted Deviates (MSWD), a measure of the deviation of the data points from the regression line that is strongly controlled by calculated uncertainties and error correlations.

#### 4. Results

The sampled units from the Ipubi Formation black shales possess between 23.8 and 45.8 % of  $\text{CaCO}_3$ , 5.1 and 18.3 % of organic matter (OM), and 4802.9 and 64566.5 ppm of Al (Table 1). Black shale interbedded marl samples possess the highest  $\text{CaCO}_3$  and lowest Al contents (Table 1). The total Re, total Os and  $^{192}\text{Os}$  (best estimate of hydrogenous osmium) concentrations for the Ipubi Formation black shales sequence are 0.61-33.73 ppb, 26.8-273.5 ppt, and 8.6-76.6 ppt, respectively (Table 1). Both Re and Os are enriched, except for the Os abundance for sample TM07, compared to the upper continental crust (0.2-2 ppb Re and 30-50 ppt Os; Esser and Turekian, 1993; Sun et al., 2003). The enrichment factor (EF) value for Re and  $^{192}\text{Os}$  ranges between 0.69 and 378.29, and 440.53 and 28062.1, respectively (Table 1). An enrichment factor greater than 1 is considered to indicate that the element is enriched relative to that of average shale, with an enrichment factor less than 1 being depleted (Tribovillard et al., 2006). Given this principle, only sample TM09 from Ipubi Formation black shale is depleted in Re, with all black shale interbedded marl samples exhibiting the highest level of enrichment in both Re and  $^{192}\text{Os}$  (Table 1). In order to allow a direct comparison of hydrogenous Os concentrations in the different samples, the  $^{192}\text{Os}$  abundance is used to avoid the addition of radiogenic  $^{187}\text{Os}$  from  $^{187}\text{Re}$  decay following deposition. A broad positive correlation exists between  $^{192}\text{Os}$  ( $r = 0.75$ ) and Re ( $r = 0.65$ ) and OM elemental, and enrichment factor values with OM (Fig. 5), suggesting an uptake mechanism that is possibly linked to the abundance of organic matter (Georgiev et al., 2012; Rooney et al., 2012). Although, a correlation between OM and Re and  $^{192}\text{Os}$  is

not always observed (Rotich et al., 2020 and references therein). In case of the Ipubi Formation black shales, the broad relationship between OM and Re and  $^{192}\text{Os}$  may also suggest that the samples were not affected by oxidative weathering, particularly as the  $\text{Os}_i$  values for Ipubi Formation black shales are positive (Table 1), which has been suggested to not indicate disturbance to the Re-Os system through oxidative weathering (Jaffe et al., 2002; Georgiev et al., 2012).

The  $^{187}\text{Re}/^{188}\text{Os}$  (85.5 to 875.6) values positively correlate with their corresponding  $^{187}\text{Os}/^{188}\text{Os}$  (1.922 to 3.757) compositions (Table 1). Regression of all the Re-Os isotope data using the Isoplot program (Ludwig, 2012) yields a Model 3 (discussed above) isochron age of  $130.22 \pm 12.57$  (12.59 - bracketed value here and below includes uncertainty in the decay constant) Ma ( $n = 9$ ; Mean Square of Weighted Deviates [MSWD] = 58.5), with an  $\text{Os}_i$  of  $1.91 \pm 0.11$  (Fig. 6). An essentially identical age ( $130.2 \pm 11.68$  [11.69] Ma) and  $\text{Os}_i$  ( $1.91 \pm 0.10$ ) is determined from the beta version of the Isochron program, which incorporates a new approach that employs the Monte Carlo sampling method for error propagation (Li et al., 2019) and the benchmark Isoplot algorithm (Ludwig, 2012), except that the uncertainty in the age is slightly smaller, but the Monte Carlo approach highlights that 80% of the uncertainty relates to the model age calculation (Fig. 6). This uncertainty was also shown by the Re-Os data of organic-rich rocks of the Green River Formation, USA (Pietras et al., 2020) and East Coast Basin, New Zealand (Rotich et al., 2020).

## 5. Discussion

### 5.1 Re-Os isotopic systematics of the black shales from Ipubi Formation

The application of the Re-Os geochronometer has permitted the determination of accurate and precise depositional ages for lacustrine, fluvio-deltaic and marine organic-rich sedimentary rocks (e.g., Ravizza and Turekian, 1989; Cohen et al., 1999; Kendall et al., 2004; Selby and Creaser, 2005b; Kendall et al., 2006; Selby, 2007; Creaser et al., 2008; Kendall et al., 2009a; Selby et al., 2009; Yang et al., 2009; Poirier and Hillaire-Marcel, 2009, 2011; Baioumy et al., 2011; Cumming et al., 2012; Cumming et al., 2013; Tripathy and Singh, 2015; Xu et al., 2017; Pietras et al., 2020). Given the chalcophilic, siderophilic, and organophilic behaviour of Re and Os, they are found primarily in organic and sulphide phases. In organic-bearing sedimentary units Re and Os has been shown to be hydrogenous (derived from sequestration from the water



column of the depositional setting) and primarily associated with/bound to organic matter (Ravizza and Turekian, 1989; Cohen et al., 1999; Selby and Creaser, 2003; Morford et al., 2005; Georgiev et al., 2011; Rooney et al., 2012).

As for other geochronological methods (e.g., Sm-Nd, Rb-Sr), the Re-Os chronometer utilizes the isochron technique to form a best-fit line of the  $^{187}\text{Re}/^{188}\text{Os}$  vs  $^{187}\text{Os}/^{188}\text{Os}$  data from an isochronous dataset. The degree of fit to the best fit line depends on the uncertainties associated with the Re and Os data (York, 1969) and are represented as a model classification (1, 2 or 3) that is based on the MSWD (reduced  $R^2$  parameter; Ludwig, 2003). ~~A Model 1 best fit of the data only takes into consideration the assigned uncertainties, whereas a Model 2 best fit assigns equal weights and zero error correlations to each point, and Model 3 best fit presumes that the scatter is due to a combination of the assigned uncertainties and an unknown but normally distributed variation in the ordinate axis values.~~

Collectively both the Isoplot (Model 3 and high MSWD = ~58) and Monte Carlo (~80% of the uncertainty derived from the model age calculation) approaches highlight that all the Re-Os data do not fully satisfy the requirements to develop a precise isochron (Fig. 6A and 6B). The uncertainty in the Re-Os age (~12 myr) and the high MSWD value (~58, higher than the ideal value of ~1) determined from all the Re-Os data ( $n = 9$ ) suggests that geological factors are the cause of the scatter of the data from the best-fit line. This could relate to the sample set possessing variable initial  $^{187}\text{Os}/^{188}\text{Os}$  and/or post-depositional disturbance to the Re-Os systematics that could be related to fracturing and gypsum veining that were present in some trenches (Yang et al., 2009; Kendall et al., 2009b; Tripathy et al., 2014). A possible explanation for the high MSWD value for the best fit of all the Re-Os data for the nine samples from Ipubi Formation black shales is demonstrated by the range in the  $\text{Os}_i$  at 130 Ma (1.74 to 1.98; Table 1). For eight of the nine samples the calculated individual initial  $^{187}\text{Os}/^{188}\text{Os}$  compositions at 130 Ma range from 1.86 to 1.98 (individual uncertainties are  $\pm 0.02 - 0.03$ ; Table 1). Sample TM09 yields a distinct initial  $^{187}\text{Os}/^{188}\text{Os}$  value of 1.74 at 130 Ma. This sample exhibits the largest deviation from the 130 Ma best fit line of 8.3 %, whereas the other samples deviate between 0.3 and 2.1 %. Sample TM09 possesses an enrichment factor for Re of 0.69 suggesting that Re is depleted relative to the average upper continental crust in this sample, which may explain its deviation in the isochron or that the water column  $^{187}\text{Os}/^{188}\text{Os}$  composition at the time of sediment deposition fluctuated across the

sampld interval. Regression of the Re-Os data without sample TM09 yields a much more precise Isoplot Model 3 age of  $124.7 \pm 5.90$  [5.93] Ma (initial  $^{187}\text{Os}/^{188}\text{Os} = 1.97 \pm 0.05$ , MSWD = 16.9) (Fig. 6C). This determined age is essentially identical to the Monte Carlo approach ( $124.7 \pm 5.63$  [5.66]; initial  $^{187}\text{Os}/^{188}\text{Os} = 1.97 \pm 0.05$ ) which also highlights that the age uncertainty is now more controlled (30 %) by the analytical uncertainty in the data (Fig. 6D). Although this Re-Os age is more precise, scatter about the best-fit line is still evident from the MSWD value of  $\sim 17$ , and that uncertainties in the model age calculation control the overall uncertainty in the derived age. Sample TM05 exhibits the largest deviation (1.9 %) from the  $\sim 125$  Ma line of best-fit, whereas the other samples deviate only between 0.1 and 0.9 %. This deviation is also highlighted by sample TM05 possessing a distinct initial  $^{187}\text{Os}/^{188}\text{Os}$  value of 2.03 at 125 Ma, whereas the other samples (with the exception of TM09) yield an average initial  $^{187}\text{Os}/^{188}\text{Os}$  value of 1.97 at 125 Ma (Table 1). The Re-Os data of this study suggests that samples TM05 and TM09 possess different  $\text{Os}_i$  compositions to that of the remaining sample set (Table 1). Regression of the Re-Os data without samples TM05 and TM09 (Fig. 6E) yields an Isoplot Model 3 age of  $124.04 \pm 4.88$  [4.91] Ma (initial  $^{187}\text{Os}/^{188}\text{Os} = 1.96 \pm 0.05$ , MSWD = 6.6). Again, this calculated age is essentially identical to the Monte Carlo approach ( $123.99 \pm 4.65$  [4.68]; initial  $^{187}\text{Os}/^{188}\text{Os} = 1.97 \pm 0.05$ ) and further shows that the age uncertainty is almost controlled equally between analytical and calculated model age uncertainties (Fig. 6F). Again, although this Re-Os age is more precise, scatter about the best-fit line is still evident from the MSWD value of 6.6 (still higher than the ideal value of  $\sim 1$ ), and that uncertainties in the model age calculation control the overall uncertainty in the derived age. Sample TM06 exhibits the largest deviation from the linear regression (0.8 %; Fig. 6E), and exhibits a nominally more radiogenic initial  $^{187}\text{Os}/^{188}\text{Os}$  composition ( $2.00 \pm 0.02$ ) in comparison to the remaining samples (TM01-04, TM07-08;  $\text{Os}_i = 1.95\text{-}1.98 \pm 0.02 - 0.03$  [average  $1.96 \pm 0.01$  1 S.D.]; Table 1).

~~The isochron approach requires that the Re-Os systematics of the sample set meet the following criteria: (i) possess identical initial  $^{187}\text{Os}/^{188}\text{Os}$  ratios, (ii) exhibit sufficient spread in  $^{187}\text{Re}/^{188}\text{Os}$  ratios of at least a few hundred units, and (iii) the Re-Os systematics remain undisturbed (Cohen et al., 1999; Selby and Creaser, 2005a). Hence, the Ipubi Formation black shales show the  $\text{Os}_i$  at 123 Ma range from 1.75 to 2.05 (Table 4). The Re-Os data of this study shows that samples TM05, TM06 and TM09 possess~~



different Os<sub>i</sub> compositions to that of the remaining sample set (Table 1). Regression of the Re-Os data without TM05, TM06 and TM09 yields an Isoplot Model 1 age of  $122.87 \pm 1.53$  [1.58] Ma (initial  $^{187}\text{Os}/^{188}\text{Os} = 1.97 \pm 0.02$ , MSWD = 1.04; Fig. 6G). Again, this calculated age is essentially identical to the Monte Carlo approach ( $122.61 \pm 3.50$  [3.52]; initial  $^{187}\text{Os}/^{188}\text{Os} = 1.97 \pm 0.02$ ) and shows that the age uncertainty is more controlled (60 %) by the analytical uncertainties than the calculated model age uncertainties (Fig. 6H). Moreover, the greater uncertainty in the age derived by the Monte Carlo approach ( $\pm 3.50$  [3.52]; Ma) further illustrates that a Model 1 Isoplot outcome underestimates the total age uncertainty arising from only considering analytical uncertainties (Li et al., 2019).

Given the isochronous behavior of the Re-Os data for six of the nine samples, which possess very similar initial  $^{187}\text{Os}/^{188}\text{Os}$  composition, the moderate different initial  $^{187}\text{Os}/^{188}\text{Os}$  values of TM05, TM06 and TM09 are considered to reflect changes in the  $^{187}\text{Os}/^{188}\text{Os}$  composition of the water column during deposition rather than disturbance to the Re-Os systematics. Here, we consider the best estimate of the depositional age of the Ipubi Formation black shales to be  $122.61 \pm 3.50$  [3.52] Ma.

The Re-Os age of ~123 Ma the Ipubi Formation black shales suggests that the studied samples were deposited during the latest Barremian/earliest Aptian. The new Re-Os age provides a significant improvement to the previous age determinations of Aptian to Albian (125 – 100.5 Ma) defined by relative dating age methods (Fig. 3; Coimbra et al., 2002; Tomé et al., 2014). Further, including the Re-Os age uncertainty, the Ipubi Formation black shale represents deposition just prior to the onset of OAE 1a (Arthur et al., 1990; Tejada et al., 2009; Jenkys, 2010). Moreover, this study suggests that, among the formations that constitute the Santana Group in the Araripe Basin, only the Romualdo (calciferous mudstone and sandstone) and Ipubi (black shales and evaporites) formations could be placed in the Aptian-Albian interval, whereas the Crato (calcareous rocks) and Barbalha (sandstone and mudstone) formations are older than the earliest Aptian (Fig. 2, 7). The latter age interval is emphasized by both palynological (e.g., *Afropollis jardinus*, *Classopollis classoides*) and ostracodal (e.g., *Damonella ultima*, *Damonella tinkoussouensis*) assemblages found in Santana Group (Coimbra et al., 2002; Neumann et al., 2003; Tomé et al., 2014; Nascimento et al., 2017), which are the same species found in Late Barremian successions worldwide (Hughes and McDougall, 1990; Bate, 1999; Gómez et al., 2001; Vallati, 2013).

389

390       5.2 ~~The beginning~~ *Insights into the timing of the marine incursion in the Araripe*  
 391 *Basin*

392       The timing of the marine incursion in the Araripe Basin is extensively debated. Among  
 393       the proposals, it is considered that the deposits of the Romualdo Formation (calciferous  
 394       mudstone and sandstone) are the first records of a marine incursion in the Araripe Basin  
 395       based on the presence of marine fossils (fishes, ostracods, gastropods, dinoflagellates  
 396       and microforaminiferal linings; Lima, 1978; Arai and Coimbra, 1990; Maisey, 2000;  
 397       Bruno and Hessel, 2006; Pereira et al., 2016) and facies associations (depositional  
 398       sequences comprising transgressive and highstand system tracts; Assine, 2007; Rojas,  
 399       2009; Assine et al., 2014; Neumann and Assine, 2015; Custódio et al., 2017). Evidence  
 400       for marine incursion during the deposition of the Ipubi Formation black shales is based  
 401       on the occurrence of both dinoflagellates (*Spinierites* and *Subtilisphaera*; Arai and  
 402       Coimbra, 1990) and palynoforaminifers (organic linings and allied material; Lima 1978;  
 403       Arai, 2012; Goldberg et al., 2019), odd-to-even *n*-alkanes distribution (Silva et al.,  
 404       2014), N/Vi ratios (0.13-0.49; Lúcio et al., 2016b) and Type II kerogen (Menezes,  
 405       2017). Further, some paleoceanographic/geographic reconstructions suggest that the  
 406       Araripe Basin was, in part, based on the presence of microfossils (noted above), a  
 407       significantly restricted NW-SE oriented marine basin that received incursion of the  
 408       Western Tethys Sea via the northeastern Brazilian São Luís and Parnáiba basins (Arai,  
 409       2014) (Fig. 8). In contrast, based on paleocurrent measurements in the Araripe and  
 410       Tucano basins, a marine incursion into the Araripe Basin is also argued to have  
 411       occurred from the south from the Proto South Atlantic (Assine et al., 2014; 2016).

412       The present-day open ocean  $^{187}\text{Os}/^{188}\text{Os}$  composition of  $\sim 1.06$  reflects the balance of  
 413       inputs between radiogenic sources (average  $^{187}\text{Os}/^{188}\text{Os}$  composition of the weathering  
 414       of upper continental crust via riverine input,  $\sim 1.4$ ) and non-radiogenic sources  
 415       ( $^{187}\text{Os}/^{188}\text{Os} \sim 0.13$ ; cosmic dust, hydrothermal fluids, and weathering of mafic or  
 416       ultramafic rocks; Esser and Turekian, 1993; Levasseur et al., 1998; Sharma et al., 1999;  
 417       Woodhouse et al., 1999; Peucker-Ehrenbrink and Ravizza, 2000; Hannah et al., 2004).  
 418       The current best estimate for the Late Barremian to Early Aptian (age of the Ipubi  
 419       Formation black shales) open ocean  $^{187}\text{Os}/^{188}\text{Os}$  composition is  $\sim 0.6$  to  $0.7$  (Tejada et  
 420       al., 2009; Bottini et al., 2012).

In lacustrine, fluvio-deltaic and restricted marine depositional settings the  $^{187}\text{Os}/^{188}\text{Os}$  value of the water column can be highly radiogenic, e.g.,  $\geq 1.0$  to 7.8 (Peucker-Ehrenbrink and Ravizza, 1996; Creaser et al., 2008; Poirier and Hillaire-Marcel, 2009, 2011; Baïoumy et al., 2011; Cumming et al., 2012; Du Vivier et al., 2014; Tripathy et al., 2015; Xu et al., 2017; Pietras et al., 2020). Given the difference between the highly radiogenic  $^{187}\text{Os}/^{188}\text{Os}$  value (1.75-2.05 at 123 Ma; Table 1) of the Ipubi Formation black shales to that of the Late Barremian to Early Aptian open ocean ( $\sim 0.6 - 0.7$ ) the initial  $^{187}\text{Os}/^{188}\text{Os}$  data would suggest a predominantly continental source for Os to the Araripe Basin from the weathering of basin adjacent Proterozoic to Archean igneous, metaigneous and metasedimentary units (Silva et al., 1997; Fetter et al., 1999; Sato et al., 2012; Ancelmi, 2016; Martins, 2017; Vale, 2018). Therefore, based on our  $\text{Os}_i$  values (average of 1.97 without TM05, TM06 and TM09 samples), coupled with biostratigraphy, organic and inorganic geochemistry and paleoceanographic reconstructions outlined above, we propose that the water mass associated with the deposition of the Ipubi Formation black shales during the Barremian/Aptian boundary was highly restricted. ~~and, probably, would have received its marine influence from the western Tethyan Sea, as proposed by Arai (2014).~~

## 6. Conclusions

This study provides the first absolute time constraints for the Ipubi Formation black shales of the Santana Group at  $123 \pm 3.5$  Ma. The age derived from Re-Os geochronology constrains deposition to the latest Barremian to the earliest Aptian, nominally prior to the onset of OAE 1a. The highly radiogenic initial  $^{187}\text{Os}/^{188}\text{Os}$  composition (1.75 - 2.054) of the Ipubi Formation black shales coupled with widely recognized paleontological, geochemical evidence, together with paleoceanographic reconstructions, suggests that the Araripe Basin was a highly restricted water mass that was also marine influenced ~~and would have received its marine influence from the western Tethys Sea.~~ The latter is in temporal agreement with a global eustasy rise during the Mid Cretaceous.

## Acknowledgements

We gratefully acknowledge Petrobras (Agreement N° 25, Cooperation term 0050.0023165.06.4) and PRH-26 (Human Resources Program of the AnP: process number 48610.013803/2009-19) for research funding. TL and JASN are grateful to the mining engineer Flávia Bastos from Campevi Mine for mine access and assistance during the sampling, and to Dr. Juliana Marques Charão for advices concerning sampling. JASN is also grateful to CNPq for his research grant (process number 312.275/2017-0). DS acknowledges the TOTAL Endowment Fund and the Dida Scholarship (CUG Wuhan) and Antonia Hoffman, Geoff Nowell, and Chris Ottley for analytical support.

## References

- Algeo, T.J., Maynard, J.B., 2004. Trace-element behavior and redox facies in core shales of Upper Pennsylvanian Kansas-type cyclothems. *Chemical Geology* 206, 289-318. <https://doi.org/10.1016/j.chemgeo.2003.12.009>
- Ancelmi, M.F., 2016. Geocronologia e geoquímica das rochas arqueanas do Complexo Granjeiro, Província da Borborema (PhD thesis). Universidade Estadual de Campinas, 159 pp. <http://repositorio.unicamp.br/handle/REPOSIP/330571>
- Antonietto, L.S., Gobbo, S.R., Carmo, D.A., Assine, M.L., Fernandes, M.A.M.C.C., Lima, J.E., 2012. Taxonomy, Ontogeny and Paleoecology of Two Species of *Harbinia* TSAO, 1959 (Crustacea, Ostracoda) from the Santana Formation, Lower Cretaceous, Northeastern Brazil. *Journal of Paleontology* 86, 659-668. <http://dx.doi.org/10.1666/11-012R.1>
- Arai M., 2012. Evidência micropaleontológica da ingressão marinha aptiana (pré-evaporítica) na Bacia do Araripe, Nordeste do Brasil. 46° Congresso Brasileiro de Geologia, Santos, Brasil. [https://www.researchgate.net/publication/301302246\\_Evidencia\\_micropaleontologica\\_da\\_ingressao\\_marinha\\_apitiana\\_pre-evaporitica\\_na\\_Bacia\\_do\\_Araripe\\_Nordeste\\_do\\_Brasil](https://www.researchgate.net/publication/301302246_Evidencia_micropaleontologica_da_ingressao_marinha_apitiana_pre-evaporitica_na_Bacia_do_Araripe_Nordeste_do_Brasil)
- Arai M., Coimbra J.C., 1990. Análise paleoecológica do registro das primeiras ingressões marinhas na Formação Santana (Cretáceo Inferior da Chapada do Araripe). 1° Simpósio da Bacia do Araripe e Bacias Interiores do Nordeste. [https://www.researchgate.net/publication/285667590\\_Analise\\_paleoecologica\\_do\\_regis](https://www.researchgate.net/publication/285667590_Analise_paleoecologica_do_regis)

- tro\_das\_primeiras\_ingressoes\_marinhas\_na\_Formacao\_Santana\_Cretaceo\_Inferior\_da\_Chapada\_do\_Araripe
- Arai, M., 2014. Aptian/Albian (Early Cretaceous) paleogeography of the South Atlantic: A paleontological perspective. *Brazilian Journal of Geology* 44 (2), 339-350. <http://dx.doi.org/10.5327/Z2317-4889201400020012>
- Arthur M.A., Brumsack H.J., Jenkyns H.C., Schlanger S.O., 1990. Stratigraphy, Geochemistry, and Paleooceanography of Organic Carbon-Rich Cretaceous Sequences. In: Ginsburg R.N., Beaudoin B. (Eds.), *Cretaceous Resources, Events and Rhythms*. NATO ASI Series (Series C: Mathematical and Physical Sciences), 304. Springer, Dordrecht, 75-119. [https://doi.org/10.1007/978-94-015-6861-6\\_6](https://doi.org/10.1007/978-94-015-6861-6_6)
- Assine, M.L., 1992. Análise estratigráfica da Bacia do Araripe, nordeste do Brasil. *Revista Brasileira de Geociências* 22, 289-300. <http://dx.doi.org/10.25249/0375-7536.1992289300>
- Assine, M.L., 2007. Bacia do Araripe. *Boletim de Geociências da Petrobras* 5, 371-389. [https://www.researchgate.net/publication/279556073\\_Araripe\\_basin\\_Bacia\\_do\\_Araripe](https://www.researchgate.net/publication/279556073_Araripe_basin_Bacia_do_Araripe)
- Assine, M.L., Perinotto, J.A.J., Custódio, M.A., Neumann, V.H., Varejão, F.G., Mescolotti, P.C., 2014. Sequências deposicionais do Andar Alagoas da Bacia do Araripe, Nordeste do Brasil. *Boletim de Geociências da Petrobras* 22 (1), 3-28. [https://www.researchgate.net/publication/311680092\\_Sequencias\\_Deposicionais\\_do\\_Andar\\_Alagoas\\_Aptiano\\_superior\\_da\\_Bacia\\_do\\_Araripe\\_Nordeste\\_do\\_Brasil](https://www.researchgate.net/publication/311680092_Sequencias_Deposicionais_do_Andar_Alagoas_Aptiano_superior_da_Bacia_do_Araripe_Nordeste_do_Brasil)
- Baioumy, H.M., Eglinton, L.B., Peucker-Ehrenbrink, B., 2011. Rhenium-osmium isotope and platinum group element systematics of marine vs. non-marine organic-rich sediments and coals from Egypt. *Chemical Geology* 285, 70-81. <https://doi.org/10.1016/j.chemgeo.2011.02.026>
- Bate, R.H., 1999. Non-marine ostracod assemblages of the Pre-salt rift basins of West Africa and their role in sequence stratigraphy. In: Cameron, N.R., Bate, R.H., Clure, V.S. (Eds.), *The Oil and Gas Habitats of the South Atlantic*. Geological Society of London. Special publication, 283-292. <http://dx.doi.org/10.1144/GSL.SP.1999.153.01.17>

- Batten, D., 2007. Spores and pollen from the Crato Formation: Biostratigraphic and palaeoenvironmental implications. In: Martill, D.M., Bechly, G., Loveridge, R. (Eds.), The Crato Fossil Beds of Brazil: Window into an Ancient World. Cambridge: Cambridge University Press, 566-574. <https://doi.org/10.1017/CBO9780511535512.021>
- Beurlen, K., 1964. As espécies dos Cassiopinae, nova subfamília dos Turritellidae, no Cretáceo do Brasil. Arquivo de Geologia [UFPE] 5, 1-43. [https://www.researchgate.net/publication/285317467\\_As\\_especies\\_dos\\_Cassiopinae\\_no\\_va\\_subfamilia\\_dos\\_Turritellidae\\_no\\_Cretaceo\\_do\\_Brasil](https://www.researchgate.net/publication/285317467_As_especies_dos_Cassiopinae_no_va_subfamilia_dos_Turritellidae_no_Cretaceo_do_Brasil)
- Beurlen, K., 1971. Bacias sedimentares do Bloco Brasileiro. Estudos Sedimentológicos 1(2), 9-31.
- Bobco, F.E.R., Goldberg, K., Bardola, T.P., 2017. Modelo deposicional do Membro Ipubi (Bacia do Araripe, nordeste do Brasil) a partir da caracterização faciológica, petrográfica e isotópica dos evaporitos. Pesquisas em Geociências 44(3), 431-451. <https://doi.org/10.22456/1807-9806.83267>
- Bottini, C., Cohen, A.S., Erba, E., Jenkyns, H.C., Coe, A.L., 2012. Osmium-isotope evidence for volcanism, weathering, and ocean mixing during the early Aptian OAE 1a. Geology 40(7), 583-586. <https://dx.doi.org/10.1130/G33140.1>
- Bruno, A.P.S., Hessel, M.H., 2006. Registros paleontológicos do cretáceo marinho na Bacia do Araripe. Estudos Geológicos 16 (1), 30-49. <https://www3.ufpe.br/estudosgeologicos/paginas/edicoes/2006161/2006161t03.pdf>
- Castro, R.G., Silva-Santos, T.L., Fambrini, G.L., Souza Neto, J.A., Pereira, R., 2017. Caracterização geoquímica da matéria orgânica dos folhelhos betuminosos na Formação Ipubi, Bacia do Araripe, NE Brasil. Geochimica Brasiliensis 31 (1), 11-27. <http://dx.doi.org/10.21715/GB2358-2812.2017301011>
- Cohen, A.S., Coe, A.L., Bartlett, J.M., Hawkesworth, C.J., 1999. Precise Re-Os ages of organic-rich mudrocks and the Os isotope composition of Jurassic seawater. Earth and Planetary Science Letters 167, 159-173. [https://doi.org/10.1016/S0012-821X\(99\)00026-6](https://doi.org/10.1016/S0012-821X(99)00026-6)

- 539 Coimbra, J.C., Arai, M., Carreño, A.L., 2002. Biostratigraphy of Lower Cretaceous  
540 Microfossils from the Araripe Basin, northeastern Brazil. *Geobios* 35, 687-698.  
541 [https://doi.org/10.1016/S0016-6995\(02\)00082-7](https://doi.org/10.1016/S0016-6995(02)00082-7)
- 542 Creaser, R., Szatmari, P., Milani, E.J., 2008. Extending Re-Os shale geochronology to  
543 lacustrine depositional systems: A case study from the major hydrocarbon source rocks  
544 of the Brazilian Mesozoic marginal basins. 33<sup>rd</sup> International Geological Congress,  
545 Oslo.
- 546 Creaser, R.A., Papanastassiou, D.A., Wasserburg, G.J., 1991. Negative thermal ion  
547 mass spectrometry of osmium, rhenium and iridium. *Geochimica et Cosmochimica*  
548 *Acta* 55, 397-401. [https://doi.org/10.1016/0016-7037\(91\)90427-7](https://doi.org/10.1016/0016-7037(91)90427-7)
- 549 Cumming, V.M., Poulton, S.W., Rooney, A.D., Selby, D., 2013. Anoxia in the  
550 terrestrial environment during the late Mesoproterozoic. *Geology* 41 (5) 583–586.  
551 <https://doi.org/10.1130/G34299.1>
- 552 Cumming, V.M., Selby, D., Lillis, P.G., 2012. Re-Os geochronology of the lacustrine  
553 Green River Formation: Insights into direct depositional dating of lacustrine  
554 successions, Re-Os systematics and paleocontinental weathering. *Earth and Planetary*  
555 *Science Letters* 359-360, 194-205. <https://doi.org/10.1016/j.epsl.2012.10.012>
- 556 Custódio, M.A., Quaglio, F., Warren, L.V., Simões, M.G., Fürsich, F.T., Perinotto,  
557 J.A.J., Assine, M.L., 2017. The transgressive-regressive cycle of the Romualdo  
558 Formation (Araripe Basin): Sedimentary archive of the Early Cretaceous marine  
559 ingression in the interior of northeast Brazil. *Sedimentary Geology* 359, 1-15.  
560 <https://doi.org/10.1016/j.sedgeo.2017.07.010>
- 561 Davis, S.P; Martill, M., 1999. The gonorynchiform fish *Dastilbe* from the Lower  
562 Cretaceous of Brazil. *Palaeontology* 42 (4), 715-740. [https://doi.org/10.1111/1475-](https://doi.org/10.1111/1475-4983.00094)  
563 [4983.00094](https://doi.org/10.1111/1475-4983.00094)
- 564 Du Vivier, A., Selby, D., Sageman, B., Jarvis, I., Grocke, D., Voigt, S., 2014. Marine  
565 <sup>187</sup>Os/<sup>188</sup>Os isotope stratigraphy reveals the interaction of volcanism and ocean  
566 circulation during Oceanic Anoxic Event 2. *Earth and Planetary Science Letters* 389,  
567 23-33. <https://doi.org/10.1016/j.epsl.2013.12.024>



- 568 Esser, B.K., Turekian, K.K., 1993. The osmium isotopic composition of the continental  
569 crust. *Geochimica et Cosmochimica Acta* 57, 3093-3104. [https://doi.org/10.1016/0016-](https://doi.org/10.1016/0016-7037(93)90296-9)  
570 7037(93)90296-9
- 571 Fabin, C.E., Correia Filho, O.J., Alencar, M.L., Barbosa, J.A., Miranda, T.S., Neumann,  
572 V.H., Gomes, I.F., Santana, F.R., 2018. Stratigraphic Relations of the Ipubi Formation:  
573 Siliciclastic-Evaporitic Succession of the Araripe Basin. *Anais da Academia Brasileira*  
574 *de Ciências* 90(2), 2049-2071. <https://doi.org/10.1590/0001-3765201820170526>
- 575 Fambrini, G.L., Silvestre, D.C., Menezes-Filho, J.A.B., Costa, I.C., Neumann,  
576 V.H.M.L., 2019. Architectural and facies characterization of the Aptian fluvial Barbalha  
577 Formation, Araripe Basin, NE Brazil. *Geological Society, London, Special Publications*  
578 488, 119-150. <https://doi.org/10.1144/SP488-2017-275>
- 579 Fetter, A.H., Van Schmus, W.R, Santos, T.J.S., Nogueira Neto, J.A., Arthaud, M.H.  
580 2000. U-Pb and Sm-Nd geochronological constraints on the crustal evolution and  
581 basement architecture of Ceará State, NW Borborema Province, NE Brazil: implications  
582 for the existence of the Paleoproterozoic Supercontinent "Atlantica". *Revista Brasileira*  
583 *de Geociências* 30(1), 102-106.  
584 <http://www.ppegeo.igc.usp.br/index.php/rbg/article/view/10928>
- 585 Field, G.J., Martill, D.M., 2017. Unusual soft tissue preservation in the Early  
586 Cretaceous (Aptian) crocodile cf. *Susisuchus* from the Crato Formation of north east  
587 Brazil. *Cretaceous Research* 75, 179-192. <https://doi.org/10.1016/j.cretres.2017.04.001>
- 588 Frey, E., Martill, D.M., Buchy, M.C., 2003. A new crested ornithocheirid from the  
589 Lower Cretaceous of northeastern Brazil and the unusual death of an unusual pterosaur.  
590 In: Buffetaut, E., Mazin, J.M. (Eds.), *Evolution and Palaeobiology of Pterosaurs* 217.  
591 *Geological Society, London, Special Publications*, 55-63.  
592 <https://doi.org/10.1144/GSL.SP.2003.217.01.05>
- 593 Georgiev, S., Stein, H.J., Hannah, J.L., Bingen, B., Weiss, H.M., Piasecki, S., 2011. Hot  
594 acidic Late Permian seas stifled life in record time. *Earth and Planetary Science Letters*  
595 310, 389–400. <https://doi.org/10.1016/j.epsl.2011.08.010>
- 596 Georgiev S., Stein H., Hannah J., Weiss H., Bingen B., Xu G., Rein E., Hatlø V., Løseth  
597 H., Nali M., Piasecki S., 2012. Chemical signals for oxidative weathering predict Re–Os



- 598 isochroneity in black shales, East Greenland. *Chemical Geology* 324–325, 108–121.  
599 <https://dx.doi.org/10.1016/j.chemgeo.2012.01.003>
- 600 Goldberg, K., Premaor, E., Bardola, T., Souza, P.A., 2019. Aptian marine ingression in  
601 the Araripe Basin: Implications for paleogeographic reconstruction and evaporite  
602 accumulation. *Marine and Petroleum Geology* 107, 214–221.  
603 <https://doi.org/10.1016/j.marpetgeo.2019.05.011>
- 604 Gómez, B., Martín-Closas, C., Méon, H., Thévenard, F., Barale, G., 2001. Plant  
605 taphonomy and palaeoecology in the lacustrine Uña delta (Late Barremian, Iberian  
606 Ranges, Spain). *Palaeogeography, Palaeoclimatology, Palaeoecology* 170, 133–148.  
607 [https://doi.org/10.1016/S0031-0182\(01\)00232-2](https://doi.org/10.1016/S0031-0182(01)00232-2)
- 608 Hannah, J.L., Bekker, A., Stein, H.J., Markey, R.J., Holland, H.D., 2004. Primitive Os  
609 and 2316 Ma age for marine shale: implications for Paleoproterozoic glacial events and  
610 the rise of atmospheric oxygen. *Earth and Planetary Science Letters* 225, 43–52.  
611 <https://doi.org/10.1016/j.epsl.2004.06.013>
- 612 Hughes, N.F., McDougall, A.B., 1990. Barremian-Aptian angiospermid pollen records  
613 from southern England. *Review of Palaeobotany and Palynology* 65, 145–151.  
614 [https://doi.org/10.1016/0034-6667\(90\)90065-Q](https://doi.org/10.1016/0034-6667(90)90065-Q)
- 615 Jaffe, L.A., Peucker-Ehrenbrink, B., Petsch, S.T., 2002. Mobility of rhenium, platinum  
616 group elements and organic carbon during black shale weathering. *Earth and Planetary  
617 Science Letter* 198, 339–353. [https://doi.org/10.1016/S0012-821X\(02\)00526-5](https://doi.org/10.1016/S0012-821X(02)00526-5)
- 618 Jenkyns, H.C., 2010. Geochemistry of oceanic anoxic events. *Geochemistry,  
619 Geophysics, Geosystems* 11(3), 1–30. <https://doi.org/10.1029/2009GC002788>
- 620 Kellner, A.W.A., 1996. Remarks on Brazilian dinosaurs. *Memoirs of the Queensland  
621 Museum* 39 (3), 611–626.  
622 [https://www.researchgate.net/publication/285026172\\_Remarks\\_on\\_Brazilian\\_dinosaurs](https://www.researchgate.net/publication/285026172_Remarks_on_Brazilian_dinosaurs)
- 623 Kellner, A.W.A., 1999. Short note on a new dinosaur (Theropoda, Coelurosauria) from  
624 the Santana Formation (Romualdo Member, Albian), northeastern Brazil. *Boletim do  
625 Museu Nacional, Geologia* 49, 1–8.  
626 [https://www.researchgate.net/publication/284618038\\_Short\\_Note\\_on\\_a\\_new\\_dinosaur\\_](https://www.researchgate.net/publication/284618038_Short_Note_on_a_new_dinosaur_)

- 627 Theropoda\_Coelurosauria\_from\_the\_Santana\_Formation\_Romualdo\_Member\_Albian\_  
628 northeastern\_Brazil
- 629 Kendall B., Creaser R.A., and Selby D., 2006. Re-Os geochronology of postglacial  
630 black shales in Australia: Constraints on the timing of “Sturtian” glaciation. *Geology*  
631 34, 729-732. <https://doi.org/10.1130/G22775.1>
- 632 Kendall, B., Creaser, R.A., Calver, C.R., Raub, T.D., Evans, D.A.D., 2009a. Correlation  
633 of sturtian diamictite successions in southern Australia and northwestern Tasmania by  
634 Re-Os black shale geochronology and the ambiguity of “Sturtian”-type diamictite-cap  
635 carbonate pairs as chronostratigraphic marker horizons. *Precambrian Research* 172,  
636 301-310. <http://dx.doi.org/10.1016/j.precamres.2009.05.001>
- 637 Kendall, B., Creaser, R.A., Gordon, G.W., Anbar, A.D., 2009b. Re-Os and Mo isotope  
638 systematics of black shales from the Middle Proterozoic Velkerri and Wollongorang  
639 formations, McArthur Basin, northern Australia. *Geochimica et Cosmochimica Acta* 73,  
640 2534-2558. <https://doi.org/10.1016/j.gca.2009.02.013>
- 641 Kendall, B.S., Creaser, R.A., Ross, G.M., Selby, D., 2004. Constraints on the timing of  
642 Marinoan “Snowball Earth” glaciation by  $^{187}\text{Re}$ - $^{187}\text{Os}$  dating of a Neoproterozoic post-  
643 glacial black shale in western Canada. *Earth and Planetary Science Letters* 222, 729-  
644 740. <https://doi.org/10.1016/j.epsl.2004.04.004>
- 645 Levasseur, S., Birck, J., Allegre, C.J., 1998. Direct measurement of femtomoles of  
646 osmium and the  $^{187}\text{Os}/^{186}\text{Os}$  ratio in seawater. *Science* 282, 272-274.  
647 <https://doi.org/10.1126/science.282.5387.272>
- 648 Li, Y., Zhang, S., Hobbs, R., Caiado, C., Sprosson, A.D., Selby, D., Rooney, A.D.,  
649 2019. Monte Carlo sampling for error propagation in linear regression and applications  
650 in isochron geochronology. *Science Bulletin* 64 (3), 189-197.  
651 <https://doi.org/10.1016/j.scib.2018.12.019>
- 652 Lima, M.R., 1978. Palinologia da Formação Santana (Cretáceo do Nordeste do Brasil)  
653 (PhD thesis). São Paulo University, 335 pp. [https://doi.org/10.11606/T.44.1978.tde-](https://doi.org/10.11606/T.44.1978.tde-16112015-153709)  
654 16112015-153709

- 655 Lima, M.R., 1979. Considerações sobre a subdivisão estratigráfica da Formação  
 656 Santana Cretáceo do Nordeste do Brasil. *Revista Brasileira de Geociências* 9(2), 116-  
 657 121. <http://www.ppegeo.igc.usp.br/index.php/rbg/article/view/12366>
- 658 Lúcio, T., Almeida, C.M.T., Pacheco Filho, J.G.A., Araújo, J.C.M., Souza Neto, J.A.,  
 659 Pereira, R., 2016a. Grau de maturação dos hidrocarbonetos dos folhelhos  
 660 pirobetuminosos da Formação Ipubi, Bacia do Araripe: Um estudo integrado de  
 661 termogravimetria, cromatografia e espectroscopia na região do infravermelho. *Estudos*  
 662 *Geológicos* 26(1), 81-97. [https://doi.org/10.18190/1980-](https://doi.org/10.18190/1980-8208/estudosgeologicos.v26n1p81-97)  
 663 [8208/estudosgeologicos.v26n1p81-97](https://doi.org/10.18190/1980-8208/estudosgeologicos.v26n1p81-97)
- 664 Lúcio, T., Moura, W.A.L., Araújo, J.C.M., França, E., Souza Neto, J.A., Pereira, R.,  
 665 2016b. Geoquímica da Formação Ipubi, Bacia do Araripe, PE: aspectos da mineralogia,  
 666 paleoclima, paleoambiente e paleossalidade. XIII Congresso de Geoquímica dos  
 667 Países de Língua Portuguesa / I Workshop de Geomatématica nas Ciências da Terra,  
 668 Fortaleza, Brasil.  
 669 [https://www.researchgate.net/publication/317225587\\_Geoquimica\\_da\\_Formacao\\_Ipubi](https://www.researchgate.net/publication/317225587_Geoquimica_da_Formacao_Ipubi_Bacia_do_Araripe_PE_aspectos_da_Mineralogia_Paleoclima_Paleoambiente_e_Paleo)  
 670 [\\_Bacia\\_do\\_Araripe\\_PE\\_aspectos\\_da\\_Mineralogia\\_Paleoclima\\_Paleoambiente\\_e\\_Paleo](https://www.researchgate.net/publication/317225587_Geoquimica_da_Formacao_Ipubi_Bacia_do_Araripe_PE_aspectos_da_Mineralogia_Paleoclima_Paleoambiente_e_Paleo)  
 671 [ssalidade](https://www.researchgate.net/publication/317225587_Geoquimica_da_Formacao_Ipubi_Bacia_do_Araripe_PE_aspectos_da_Mineralogia_Paleoclima_Paleoambiente_e_Paleo)
- 672 Ludwig, K.R., 1980. Calculation of uncertainties of U-Pb isotope data. *Earth and*  
 673 *Planetary Science Letter* 46, 212-220. [https://doi.org/10.1016/0012-821X\(80\)90007-2](https://doi.org/10.1016/0012-821X(80)90007-2)
- 674 Ludwig, K.R., 2003. User's manual for Isoplot 3.00: A geochronological toolkit for  
 675 Microsoft Excel. Special publication / Berkeley Geochronology Center 4.  
 676 [https://www.researchgate.net/publication/301951506\\_User%27s\\_Manual\\_for\\_IsoplotE](https://www.researchgate.net/publication/301951506_User%27s_Manual_for_IsoplotE)  
 677 [x\\_rev\\_300\\_A\\_Geochronological\\_Toolkit\\_for\\_Microsoft\\_Excel](https://www.researchgate.net/publication/301951506_User%27s_Manual_for_IsoplotE)
- 678 Ludwig, K.R., 2012. Isoplot, version 3.75: A geochronological Toolkit for Microsoft  
 679 Excel. Berkeley Geochronology Center Special Publication No. 5.  
 680 [http://www.bgc.org/isoplot\\_etc/isoplot/Isoplot3\\_75-4\\_15manual.pdf](http://www.bgc.org/isoplot_etc/isoplot/Isoplot3_75-4_15manual.pdf)
- 681 Maisey, J.G., 2000. Continental break-up and the distribution of fishes in Western  
 682 Gondwana during the Early Cretaceous. *Cretaceous Research* 21, 281-314.  
 683 <https://doi.org/10.1006/cres.1999.0195>

- 684 Martill, D.M., Unwin, D.M., 1989. Exceptionally well preserved pterosaur wing  
685 membrane from the Cretaceous of Brazil. *Nature* 340, 138-140.  
686 <https://doi.org/10.1038/340138a0>
- 687 Martill, D.M. (Ed.), 1996. Fossils of the Santana and Crato Formations, Brazil.  
688 Palaeontological Association Field Guides to Fossils 5, 160 pp.
- 689 Martill, D.M., 2007. The age of the Cretaceous Santana Formation fossil Konservat  
690 Lagerstätte of north-east Brazil: A historical review and an appraisal of the  
691 biochronostratigraphic utility of its palaeobiota. *Cretaceous Research* 28, 895-920.  
692 <https://doi.org/10.1016/j.cretres.2007.01.002>
- 693 Martill, D.M., Bechly, G. and Loveridge, R.F. (Eds.), 2007. The Crato Fossil Beds of  
694 Brazil: Window into an Ancient World. Cambridge University Press, Cambridge, 625  
695 pp. <https://doi.org/10.1017/CBO9780511535512>
- 696 Martill, D.M., Cruickshank, A. R. I., Frey, E., Small P.G., Clarke M., 1996. A new  
697 crested maniraptoran dinosaur from the Santana Formation (Lower Cretaceous) of  
698 Brazil. *Journal of the Geological Society* 153, 5-8.  
699 <https://doi.org/10.1144/gsjgs.153.1.0005>
- 700 Martill, D.M., Frey, E., 1998. A new pterosaur Lagerstätte in N.E. Brazil (Crato  
701 Formation; Aptian, Lower Cretaceous): Preliminary observations. *Oryctos* 1, 79-85.  
702 [https://www.researchgate.net/publication/288089527\\_A\\_new\\_pterosaur\\_Lagerstatte\\_in](https://www.researchgate.net/publication/288089527_A_new_pterosaur_Lagerstatte_in_N_E_Brazil_Crato_Formation_Aptian_Lower_Cretaceous_Preliminary_observations)  
703 [\\_N\\_E\\_Brazil\\_Crato\\_Formation\\_Aptian\\_Lower\\_Cretaceous\\_Preliminary\\_observations](https://www.researchgate.net/publication/288089527_A_new_pterosaur_Lagerstatte_in_N_E_Brazil_Crato_Formation_Aptian_Lower_Cretaceous_Preliminary_observations)
- 704 Martill, D.M., Frey, E., Sues, H.D., Cruickshank, A.R.I, 2000. Skeletal remains of a  
705 small theropod dinosaur with associated soft structures from the Lower Cretaceous  
706 Santana Formation of northeastern Brazil. *Canadian Journal of Earth Sciences* 37 (6),  
707 891-900. <https://doi.org/10.1139/e00-001>
- 708 Martins, D.T., 2017. Evolução tectônica das rochas encaixantes das Formações  
709 Ferríferas Bandadas de Manga Velha-PI, Província Borborema (Unpubl. PhD thesis).  
710 Universidade Federal do Ceará, 86 pp.
- 711 Matos R.M.D., 1999. History of the northeast Brazilian rift system: kinematic  
712 implications for the break-up between Brazil and West Africa. In: Cameron, N.R., Bate,  
713 R.H., Clure, V.S. (Eds.), *The Oil and Gas Habitats of the South Atlantic*. Geological

- 714 Society, London, Special Publications 153, 55-73.  
 715 <https://doi.org/10.1144/GSL.SP.1999.153.01.04>
- 716 Matos, R.M.D., 1992. The Northeast Brazilian Rift System. *Tectonics* 11, 766-791.  
 717 <https://doi.org/10.1029/91TC03092>
- 718 Medeiros V.C., 2004. Evolução geodinâmica e condicionamento estrutural dos terrenos  
 719 Piancó-Alto Brígida e Alto Pajeú, Domínio da Zona Transversal, NE do Brasil (PhD  
 720 thesis). Federal University of Rio Grande do Norte, 200 pp.  
 721 <http://rigeo.cprm.gov.br/jspui/handle/doc/105>
- 722 Menezes, J.D.O., 2017. Geoquímica e petrografia orgânica da Formação Santana, Bacia  
 723 do Araripe, Nordeste do Brasil (PhD thesis). Federal University of Rio Grande do Sul,  
 724 75 pp. <http://hdl.handle.net/10183/156391>
- 725 Morford J.L., Emerson S.R., Breckel E.J., Hyun Kim S., 2005. Diagenesis of oxyanions  
 726 (V, U, Re and Mo) in pore waters and sediments from a continental margin. *Geochimica*  
 727 *Cosmochimica et Acta* 69, 5021-5032. <https://doi.org/10.1016/j.gca.2005.05.015>
- 728 Morford, J.L., Emerson, S., 1999. The geochemistry of redox sensitive trace metals in  
 729 sediments. *Geochimica et Cosmochimica Acta* 63, 1735-1750.  
 730 [https://doi.org/10.1016/S0016-7037\(99\)00126-X](https://doi.org/10.1016/S0016-7037(99)00126-X)
- 731 Nascimento Jr, D.R., da Silva Filho, W.F., Freire Jr, J.G., dos Santos, F.H., 2016.  
 732 Syngenetic and diagenetic features of evaporite-lutite successions of the Ipubi  
 733 Formation, Araripe Basin, Santana do Cariri, NE Brazil. *Journal of South American*  
 734 *Earth Sciences* 72, 315-327. <https://doi.org/10.1016/j.jsames.2016.10.001>
- 735 Nascimento, L.R.S.L., Tome, M.E.T.R., Barreto, A.M.F., Oliveira, D.H., Neumann,  
 736 V.H.M.L., 2017. Diagnóstico palinoflorístico do poço 2-JNS-01PE, Cretáceo Inferior,  
 737 Bacia do Jatobá, Nordeste do Brasil. *Estudo Geológicos* 27(1), 118-134. [https://](https://10.18190/1980-8208/estudosgeologicos.v27n1p118-134)  
 738 [10.18190/1980-8208/estudosgeologicos.v27n1p118-134](https://10.18190/1980-8208/estudosgeologicos.v27n1p118-134)
- 739 Neumann, V.H., Assine, M.L., 2015. Stratigraphic proposal to the post-rift I tectonic-  
 740 sedimentary sequence of Araripe Basin, Northeastern Brazil. 2nd International Congress  
 741 on Stratigraphy, Graz, Austria.

- Neumann, V.H., Borrego, A.G., Cabrera, L., Dino, R., 2003. Organic matter composition and distribution through the Aptian–Albian lacustrine sequences of the Araripe Basin, northeastern Brazil. *International Journal of Coal Geology* 54, 21-40. [https://doi.org/10.1016/S0166-5162\(03\)00018-1](https://doi.org/10.1016/S0166-5162(03)00018-1)
- Neumann, V.H., Cabrera, L., 1999. Una nueva propuesta estratigráfica para la tectonosecuencia post-rifte de la Cuenca de Araripe, noreste de Brasil. 5º Simpósio sobre o Cretáceo do Brasil / 1º Simpósio sobre el Cretácico de América del Sur, Serra Negra. Brasil. [https://www.researchgate.net/publication/285885346\\_Una\\_nueva\\_propuesta\\_estratigrafica\\_para\\_la\\_tectonosecuencia\\_post-rifte\\_de\\_la\\_cuenca\\_de\\_Araripe\\_noreste\\_de\\_Brasil](https://www.researchgate.net/publication/285885346_Una_nueva_propuesta_estratigrafica_para_la_tectonosecuencia_post-rifte_de_la_cuenca_de_Araripe_noreste_de_Brasil)
- Neumann, V.H.M.L., 1999. Estratigrafía, sedimentología, geoquímica y diagénesis de los sistemas lacustres Aptienses-Albienses de la Cuenca de Araripe (Noreste de Brasil) (Unpubl. PhD thesis). Universitat de Barcelona, 233 pp.
- Oliveira, A.A., Brito, A.L.F., Santos, M.E.C.M., Carvalho, M.S.S., 1979. Projeto Chapada Do Araripe. DNPM/CPRM Final Report 1, 123.
- Oliveira, G.R., Kellner, A.W.A., 2017. Rare hatchling specimens of *Araripemys* Price, 1973 (Testudines, Pelomedusoides, Araripemydidae) from the Crato Formation, Araripe Basin. *Journal of South American Earth Sciences* 79, 137-142. <https://doi.org/10.1016/j.jsames.2017.07.014>
- Pereira, P.A., Cassab, R.D.C.T., Barreto, A.M.F., 2016. Cassiopidae gastropods, influence of Tethys Sea of the Romualdo Formation (Aptian-Albian), Araripe Basin, Brazil. *Journal of South American Earth Sciences* 70, 211-223. <https://doi.org/10.1016/j.jsames.2016.05.005>
- Peucker-Ehrenbrink, B., Ravizza, G., 1996. Continental runoff of osmium into the Baltic Sea. *Geology* 24 (4), 327-330. [https://doi.org/10.1130/0091-7613\(1996\)024%3C0327:CROOIT%3E2.3.CO;2](https://doi.org/10.1130/0091-7613(1996)024%3C0327:CROOIT%3E2.3.CO;2)
- Peucker-Ehrenbrink, B., Ravizza, G., 2000. The marine osmium isotope record. *Terra Nova* 12, 205-219. <https://doi.org/10.1046/j.1365-3121.2000.00295.x>
- Pietras, J.T., Selby, D., Brembs, R., Dennett, A., 2020. Tracking drainage basin evolution, continental tectonics, and climate change: Implications from osmium

- isotopes of lacustrine systems. *Palaeogeography, Palaeoclimatology, Palaeoecology* 537, 109471. <https://doi.org/10.1016/j.palaeo.2019.109471>
- Poirier, A., Hillaire-Marcel, C., 2011. Improved Os-isotope stratigraphy of the Arctic Ocean. *Geophysical Research Letter* 38, 1-6. <https://doi.org/10.1029/2011GL047953>
- Poirier, A., Hillaire-Marcel, C., 2009. Os-isotope insights into major environmental changes of the Arctic Ocean during the Cenozoic. *Geophysical Research Letter* 36, 1-5. doi:10.1029/2009GL037422
- Ponte, F.C., Appi, C.J., 1990. Proposta de revisão da coluna litoestratigráfica da Bacia do Araripe. 36º Congresso Brasileiro de Geologia, Natal, Brasil, 211-226.
- Ponte, F.C., Ponte Filho, F.C., 1996. Estrutura Geológica e Evolução Tectônica da Bacia do Araripe. DNPM, Recife, 98 pp.
- Prado, L.A.C., Pereira, P.A., Sales, A.M.F., Barreto, A.M.F., 2015. Taphonomic and paleoenvironmental considerations for the concentrations of macroinvertebrate fossils in the Romualdo Member, Santana Formation, Late Aptian-Early Albian, Araripe Basin, Araripina, NE, Brazil. *Journal of South American Earth Sciences* 62, 218-228. <https://doi.org/10.1016/j.jsames.2015.06.005>
- Ravizza, G., Turekian, K.K., 1989. Application of the  $^{187}\text{Re}$ - $^{187}\text{Os}$  system to black shale geochronometry. *Geochimica et Cosmochimica Acta* 53, 3257-3262. [https://doi.org/10.1016/0016-7037\(89\)90105-1](https://doi.org/10.1016/0016-7037(89)90105-1)
- Regali, M.S.P., 1990. A idade dos evaporitos da plataforma continental do Ceará, Brasil, e sua relação com os outros evaporitos das bacias nordestinas. *Boletim do IG-USP* 7, 139-143. <https://doi.org/10.11606/issn.2317-8078.v0i7p139-143>
- Rojas, F.E.M., 2009. Estratigrafia de sequências do intervalo Aptiano ao Albiano na Bacia do Araripe, NE do Brasil (Masters dissertation). Federal University of Rio Grande do Norte, 122 pp. <http://dx.doi.org/10.1590/S0102-261X2010000100011>
- Rooney, A.D., Selby, D., Lewan, M.D., Lillis, P.G., Houzay, J.P., 2012. Evaluating Re-Os systematics in organic-rich sedimentary rocks in response to petroleum generation using hydrous pyrolysis experiments. *Geochimica et Cosmochimica Acta* 77, 275-291. <https://doi.org/10.1016/j.gca.2011.11.006>



- 801 Rotich, E.K., Handler, M.R., Naeher, S., Selby, D., Hollis, C.J., Sykes, R., 2020. Re-Os  
802 geochronology and isotope systematics, and organic and sulfur geochemistry of the  
803 middle-late Paleocene Waipawa Formation, New Zealand: Insights into early Paleogene  
804 seawater Os isotope composition. *Chemical Geology* 536, 1-18.  
805 <https://doi.org/10.1016/j.chemgeo.2020.119473>
- 806 Sato, E.N, Almeida, T.I.R., Basei, A.S., 2012. Idades U-Pb em zircões das rochas  
807 encaixantes das formações ferríferas do distrito de Curral Novo do Piauí, Brasil. 34th  
808 International Geological Congress (IGC), Austrália.
- 809 Scherer, C.M.S., Jardim de Sá, E.F., Córdoba, V.C., Sousa, D.C., Aquino, M.M.,  
810 Cardoso, F.M.C., 2014. Tectono-stratigraphic evolution of the Upper Jurassic-  
811 Neocomian rift succession, Araripe Basin, Northeast Brazil. *Journal of South American*  
812 *Earth Sciences* 49, 106-122. <https://doi.org/10.1016/j.jsames.2013.10.007>
- 813 Schweigert, G., Martill, D., Williams, M., 2007. Crustacea of the Crato Formation. In:  
814 Martill, D.M., Bechly, G., Loveridge, R. (Eds.), *The Crato Fossil Beds of Brazil:*  
815 *Window into an Ancient World*. Cambridge: Cambridge University Press, 133-141.  
816 <https://doi.org/10.1017/CBO9780511535512.011>
- 817 Scotese, C.R., 2014. Atlas of Early Cretaceous Paleogeographic Maps, PALEOMAP  
818 Atlas for ArcGIS, volume 2, The Cretaceous, Maps 23 - 31, Mollweide Projection,  
819 PALEOMAP Project, Evanston, IL. PALEOMAP Project, Evanston, IL.  
820 <https://doi.org/10.13140/2.1.4099.4560>
- 821 Scotese, C.R., Moore, T.L., 2014. Atlas of Phanerozoic Ocean Currents and Salinity  
822 (Mollweide Projection), Volumes 1-6, PALEOMAP Project PaleoAtlas for ArcGIS,  
823 PALEOMAP Project, Evanston, IL.  
824 [https://www.researchgate.net/publication/267511712\\_Atlas\\_of\\_Phanerozoic\\_Ocean\\_Cu](https://www.researchgate.net/publication/267511712_Atlas_of_Phanerozoic_Ocean_Currents_and_Salinity_Mollweide_Projection_Volumes_1-6_PALEOMAP_Project_PaleoAtlas_for_ArcGIS_PALEOMAP_Project_Evanston_IL)  
825 [rrents\\_and\\_Salinity\\_Mollweide\\_Projection\\_Volumes\\_1-](https://www.researchgate.net/publication/267511712_Atlas_of_Phanerozoic_Ocean_Currents_and_Salinity_Mollweide_Projection_Volumes_1-6_PALEOMAP_Project_PaleoAtlas_for_ArcGIS_PALEOMAP_Project_Evanston_IL)  
826 [6\\_PALEOMAP\\_Project\\_PaleoAtlas\\_for\\_ArcGIS\\_PALEOMAP\\_Project\\_Evanston\\_IL](https://www.researchgate.net/publication/267511712_Atlas_of_Phanerozoic_Ocean_Currents_and_Salinity_Mollweide_Projection_Volumes_1-6_PALEOMAP_Project_PaleoAtlas_for_ArcGIS_PALEOMAP_Project_Evanston_IL)
- 827 Selby D., Creaser R.A., 2003. Re-Os geochronology of organic rich sediments: an  
828 evaluation of organic matter analysis methods. *Chemical Geology* 200, 225-240.  
829 [https://doi.org/10.1016/S0009-2541\(03\)00199-2](https://doi.org/10.1016/S0009-2541(03)00199-2)



- 830 Selby D., Creaser R.A., 2005a. Direct radiometric dating of hydrocarbon deposits using  
831 rhenium-osmium isotopes. *Science* 308, 1293-1295.  
832 <https://doi.org/10.1126/science.1111081>
- 833 Selby D., Creaser R.A., 2005b. Direct radiometric dating of the Devonian-Mississippian  
834 time-scale boundary using the Re-Os black shale geochronometer. *Geology* 33, 545-  
835 548. <https://doi.org/10.1130/G21324.1>
- 836 Selby, D., 2007. Direct Rhenium-Osmium age of the Oxfordian-Kimmeridgian  
837 boundary, Staffin bay, Isle of Skye, U.K., and the late Jurassic time scale. *Norwegian*  
838 *Journal of Geology* 87(3), 291-299.  
839 [https://www.researchgate.net/publication/285745042\\_Direct\\_Rhenium-](https://www.researchgate.net/publication/285745042_Direct_Rhenium-Osmium_age_of_the_Oxfordian-Kimmeridgian_boundary_Staffin_bay_Isle_of_Skye_UK_and_the_Late_Jurassic_time_scale)  
840 [Osmium\\_age\\_of\\_the\\_Oxfordian-](https://www.researchgate.net/publication/285745042_Direct_Rhenium-Osmium_age_of_the_Oxfordian-Kimmeridgian_boundary_Staffin_bay_Isle_of_Skye_UK_and_the_Late_Jurassic_time_scale)  
841 [Kimmeridgian\\_boundary\\_Staffin\\_bay\\_Isle\\_of\\_Skye\\_UK\\_and\\_the\\_Late\\_Jurassic\\_time\\_](https://www.researchgate.net/publication/285745042_Direct_Rhenium-Osmium_age_of_the_Oxfordian-Kimmeridgian_boundary_Staffin_bay_Isle_of_Skye_UK_and_the_Late_Jurassic_time_scale)  
842 [scale](https://www.researchgate.net/publication/285745042_Direct_Rhenium-Osmium_age_of_the_Oxfordian-Kimmeridgian_boundary_Staffin_bay_Isle_of_Skye_UK_and_the_Late_Jurassic_time_scale)
- 843 Selby, D., Creaser, R.A., Stein, H.L., Markey, R.J., Hannah, J.L., 2007. Assessment of  
844 the  $^{187}\text{Re}$  decay constant by cross calibration of Re-Os molybdenite and U-Pb zircon  
845 chronometers in magmatic ore systems. *Geochimica et Cosmochimica Acta* 71, 1999-  
846 2013. <https://doi.org/10.1016/j.gca.2007.01.008>
- 847 Selby, D., Mutterlose, J., Condon, D.J., 2009. U-Pb And Re-Os Geochronology of the  
848 Aptian/Albian and Cenomanian/Turonian stage boundaries: Implications for timescale  
849 calibration, osmium isotope seawater composition and Re-Os systematics in organic-  
850 rich sediments. *Chemical Geology* 265, 394-409.  
851 <https://doi.org/10.1016/j.chemgeo.2009.05.005>
- 852 Sharma, M., Wasserburg, G.J., Hofmann, A.W., Chakrapani, G.J., 1999. Himalayan  
853 uplift and osmium isotopes in oceans and rivers. *Geochimica et Cosmochimica Acta* 63,  
854 4005-4012. [https://doi.org/10.1016/S0016-7037\(99\)00305-1](https://doi.org/10.1016/S0016-7037(99)00305-1)
- 855 Silva, M.A.M., 1986. Lower Cretaceous unconformity truncating evaporite-carbonate  
856 sequence, Araripe Basin, Northeastern Brazil. *Revista Brasileira de Geociências* 16(3),  
857 306-310. <http://www.ppegeo.igc.usp.br/index.php/rbg/article/view/12012>

- 858 Silva, M.D., 1975. Primeira ocorrência de charophyta na Formação Santana (Cretáceo)  
 859 do Grupo Araripe, nordeste do Brasil. VII Simpósio de Geologia do NE, Fortaleza,  
 860 Brasil, 67-73.
- 861 Silva, L.C., McNaughton, N.J., Vasconcelos, A.M., Gomes, J.R.C., Fletcher, I.R., 1997.  
 862 U-Pb SHRIMP ages in southern State of Ceará, Borborema province, NE Brazil:  
 863 Archean TTG accretion and Proterozoic crustal reworking. 2<sup>th</sup> International  
 864 Symposium on Granites and Associated Mineralizations, 280-281.
- 865 Silva, T.L.S., Mendes, P.R.C., Castro, R.G., Pereira, R., Souza Neto, J.A., Fambrini,  
 866 G.L., 2014. Caracterização geoquímica de folhelhos betuminosos da Formação Ipubi,  
 867 Bacia do Araripe por meio de *n*-alcanos e isoprenoides. 47º Congresso Brasileiro de  
 868 Geologia, Salvador, Brasil.  
 869 [https://www.researchgate.net/publication/334151694\\_CHARACTERIZACAO\\_GEOQUIMICA\\_DOS\\_FOLHELHOS\\_PIROBETUMINOSOS\\_DA\\_FORMACAO\\_IPUBI\\_BACIA\\_DO\\_ARARIPE\\_POR\\_MEIO\\_DE\\_n-ALCANOS\\_E\\_ISOPRENOIDES](https://www.researchgate.net/publication/334151694_CHARACTERIZACAO_GEOQUIMICA_DOS_FOLHELHOS_PIROBETUMINOSOS_DA_FORMACAO_IPUBI_BACIA_DO_ARARIPE_POR_MEIO_DE_n-ALCANOS_E_ISOPRENOIDES)
- 872 Silva-Telles Jr., A.C., Vianna, M.S.S., 1990. Paleoeecologia dos ostracodes da Formação  
 873 Santana (Bacia do Araripe): Um estudo ontogenético de populações. I Simpósio Bacia  
 874 Araripe e Bacias Interiores Nordeste, Crato, Brasil.
- 875 Smoliar, M.I., Walker, R.J., Morgan, J.W., 1996. Re-Os Ages of Group IIA, IIIA, IVA,  
 876 and IVB Iron Meteorites. Science 271, 1099-1102.  
 877 <https://www.jstor.org/stable/2889840>
- 878 Souza Neto, J.A., Vortisch, W.B., Mort, H.P., Valença, L.M.M., Barbosa, J.A.,  
 879 Neumann, V.H.M.L., Miranda, T.S., Correia Filho, O.J., Brandao, P.A.L.S., Moriel,  
 880 I.S., 2013. Mineralogical and chemical characterization of clay minerals filling  
 881 gypsum-rich veins crosscutting the evaporite sequence of the Ipubi Formation, Araripe  
 882 Basin, northeastern Brazil. XV International Clay Conference, Rio de Janeiro, Brasil.  
 883 [https://tiagomirandaorg.files.wordpress.com/2016/12/799\\_souza\\_neto\\_et\\_al\\_xv\\_icc\\_20](https://tiagomirandaorg.files.wordpress.com/2016/12/799_souza_neto_et_al_xv_icc_2013_fractures.pdf)  
 884 [13\\_fractures.pdf](https://tiagomirandaorg.files.wordpress.com/2016/12/799_souza_neto_et_al_xv_icc_2013_fractures.pdf)
- 885 Sucerquia, P.A., Bernardes-de-Oliveira, M.E.C., Mohr, B.A.R., 2015. Phytogeographic,  
 886 stratigraphic and paleoclimatic significance of *Pseudofrenelopsis capillata* sp. nov.  
 887 from the Lower Cretaceous Crato Formation, Brazil. Review of Palaeobotany and  
 888 Palynology 222, 116-128. <https://doi.org/10.1016/j.revpalbo.2015.07.012>

- 889 Tejada, M.L.G., Suzuki, K., Kuroda, J., Coccioni, R., Mahoney, J.J., Ohkouchi, N.,  
 890 Sakamoto, T., Tatsumi, Y., 2009. Ontong Java Plateau eruption as a trigger for the Early  
 891 Aptian oceanic anoxic event. *Geology* 37, 855-858. <https://doi.org/10.1130/G25763A.1>
- 892 Tomé, M.E.R.T., Lima Filho, M.F., Neumann, V.H.M.L., 2014. Taxonomic studies of  
 893 non-marine ostracods in the Lower Cretaceous (Aptian-Lower Albian) of post-rift  
 894 sequence from Jatobá and Araripe basins (Northeast Brazil): Stratigraphic implications.  
 895 *Cretaceous Research* 48, 153-176. <https://doi.org/10.1016/j.cretres.2013.12.007>
- 896 Tribovillard, N., Algeo, T.J., Lyons, T., Riboulleau, A., 2006. Trace metals as  
 897 paleoredox and paleoproductivity proxies: An update. *Chemical Geology* 232, 12-32.  
 898 <https://doi.org/10.1016/j.chemgeo.2006.02.012>
- 899 Tripathy, G.R., Hannah, J.L., Stein, H.J., Yang, G., 2014. Re–Os age and depositional  
 900 environment for black shales from the Cambrian–Ordovician boundary, Green Point,  
 901 western Newfoundland. *Geochem. Geophys. Geosyst.* 15, 1021–1037.  
 902 <http://dx.doi.org/10.1002/2013GC005217>.
- 903 Tripathy, G.R., Hannah, J.L., Stein, H.J., Geboy, N.J., Ruppert, L.F., 2015. Radiometric  
 904 dating of marine-influenced coal using Re–Os geochronology. *Earth and Planetary  
 905 Science Letters* 432, 13-23. <http://dx.doi.org/10.1016/j.epsl.2015.09.030>
- 906 Tripathy, G.R., Singh, S.K., 2015. Re–Os depositional age for black shales from the  
 907 Kaimur Group, Upper Vindhyan, India. *Chemical Geology* 413, 63-72.  
 908 <https://doi.org/10.1016/j.chemgeo.2015.08.011>
- 909 Unwin, D., Martill, D., 2007. Pterosaurs of the Crato Formation. In: Martill, D.M.,  
 910 Bechly, G., Loveridge, R. (Eds.), *The Crato Fossil Beds of Brazil: Window into an  
 911 Ancient World*. Cambridge: Cambridge University Press, 475-524.  
 912 <https://doi.org/10.1017/CBO9780511535512.018>
- 913 Vallati, P., 2013. A Mid-Cretaceous palynoflora with *tucanopollis crisopolensis* from  
 914 D-129 Formation, San Jorge Gulf Basin, Argentina. *Revista Brasileira de Paleontologia*  
 915 16(2), 237-244. <https://10.4072/rbp.2013.2.06>
- 916 Vale, J.A.R., 2018. Caracterização geoquímica e geocronológica do Complexo  
 917 Granjeito, Província da Borborema, NE Brasil: implicações para a evolução crustal

- paleoarqueana do distrito ferrífero de Curral Novo do Piauí (PhD thesis). Universidade de São Paulo, 131 pp. <https://doi.org/10.11606/D.44.2019.tde-30052019-103844>
- Warren, J.K. (Ed.), 2016. *Evaporites a Geological Compendium*. Springer, Switzerland, 1813 pp. <https://doi.org/10.1007/978-3-319-13512-0>
- Witton, M.P., 2007. Titans of the skies: Azhdarchid pterosaurs. *Geology Today* 23, 33-38. <https://doi.org/10.1111/j.1365-2451.2007.00596.x>
- Woodhouse, O., Ravizza, G., Falkner, K.K., Statham, P., Peucker-Ehrenbrink, B., 1999, Osmium in seawater: vertical profiles of concentration and isotopic composition in the eastern Pacific Ocean. *Earth and Planetary Science Letters*.173, 223-233. [https://doi.org/10.1016/S0012-821X\(99\)00233-2](https://doi.org/10.1016/S0012-821X(99)00233-2)
- Xu, W., Ruhl, M., Jenkyns, H.C., Hesselbo, S.P., Riding, J.B., Selby, D., Naafs, B.D.A., Weijers, J.W.H., Pancost, R.D., Tegelaar, E.W., Idiz, E.F., 2017. Carbon sequestration in an expanded lake system during the Toarcian oceanic anoxic event. *Nature Geoscience* 10, 129-134. <https://www.nature.com/articles/ngeo2871>
- Yang, G., Hannah, J., Zimmerman, A., Stein, H., Bekker, A., 2009. Re–Os depositional age for Archean carbonaceous slates from the southwestern Superior Province: challenges and insights. *Earth and Planetary Science Letters* 280, 83–92.
- York, D., 1969. Least-squares fitting of a straight line with correlated errors. *Earth and Planetary Science Letters* 5, 320-324. [https://doi.org/10.1016/S0012-821X\(68\)80059-7](https://doi.org/10.1016/S0012-821X(68)80059-7)

## FIGURE CAPTIONS

Fig. 1. Location of the Araripe Basin (highlighted by the red box) within the geotectonic context of the Borborema Province. MCD: Médio Coreaú Domain; CD: Cearence Domain; RGND: Rio Grande do Norte Domain; TZD: Transversal Zone Domain; SD: South Domain (Modified from Matos, 1999; Medeiros, 2004).

Fig. 2. Simplified map of the Araripe Basin to represent sampling location (Modified from Assine, 2007).

Fig. 3. Schematic stratigraphic profile and micropaleontology assemblage of the Santana Group, Araripe Basin (based in Coimbra et al., 2002; Tomé et al., 2014).

Fig. 4. Sampling strategy and composite stratigraphy of the 1m interval sampled of the Ipubi Formation black shale. (A and B) The Ipubi Formation black shales were exposed via nine 1 m deep trenches ~4 m apart in the open pit of the Campevi mine. (C) Composite stratigraphic section of the black shale interval exposed (see text for details). (D) Example of fibrous gypsum-filled lens in the upper interval of the black shale profile; (E) fossils within the upper interval of the stratigraphic profile; (F) 30 cm interval of black shale interbedded with marl, and (G) mudstone within the basal 20 cm of the sampled interval.

Fig. 5. Cross-plot of Re (ppb),  $^{192}\text{Os}$  (ppt), and enrichment factor of Re and  $^{192}\text{Os}$  versus organic matter for the studied samples. See text for discussion.

Fig. 6. Re-Os geochronological results for the Ipubi Formation black shales from the Campevi mine, Brazil. Regression of the Re-Os isotope data together with the  $2\sigma$  uncertainties in the isotope ratios and the associated error correlation functions ( $\rho$ ) conducted using the beta version of Isochron program (Li et al., 2019), which incorporates the Isoplot algorithm (A, C, E, G) (Ludwig, 2012) and the Monte Carlo method (B, D, F, H). Isoplot data regressions are shown for all data (A), and with only sample TM09 excluded (C), and with samples TM05 and TM09 excluded (E), and with samples TM05, TM06 and TM09 excluded (G). Monte Carlo approach distribution of age and initial  $^{187}\text{Os}/^{188}\text{Os}$  values are shown in B (all data), D (TM09 excluded), F (TM05 and TM09 excluded), and H (TM05, TM06 and TM09 excluded). The inset shows total uncertainty at the 2 sigma level and the contribution to the total uncertainty from the analytical uncertainty. Bracketed age uncertainties include the uncertainty on the decay constant. See text for discussion.

Fig. 7. A new chronostratigraphic proposal for the deposition of the lithostratigraphic units of the Post-Rift I sequence (Santana Group) of the Araripe Basin based on both regional observations (Assine et al., 2014; Neumann and Assine, 2015; Custódio et al., 2017) and the Re-Os age presented in this study.

Fig. 8. Aptian paleogeographic and paleoceanographic map illustrating the western Tethys Sea incursion in the northeast Brazilian basins. The red arrows represent the

976 paleocirculation during this period. The Araripe Basin is represented by the yellow star,  
977 and the São Luís and Parnaíba basins are represented by the purple and orange star,  
978 respectively (modified after Scotese, 2014; Scotese and Moore, 2014; Arai, 2014).

Table 1: Synopsis of organic matter, CaCO<sub>3</sub> and aluminium content, enrichment factor data, and Re-Os data for the samples from Ipubi Formation black shale.

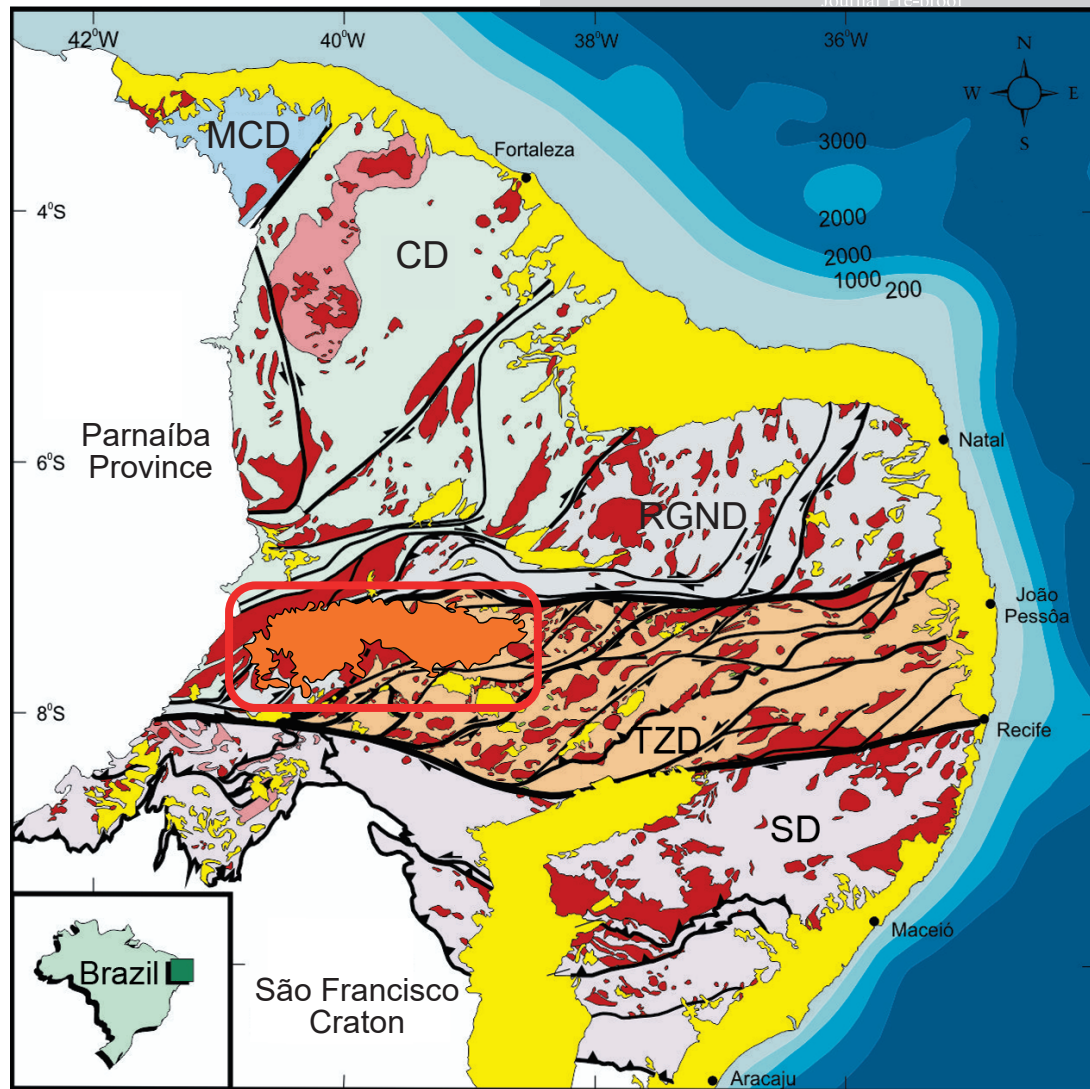
Batch/Sample	Lithology	CaCO <sub>3</sub> (%)	OM (%)	Al (ppm)	Re (EF) <sup>#</sup>	<sup>192</sup> Os (EF) <sup>#</sup>	Re (ppb)	±	Os (ppt) <sup>^</sup>	±	<sup>192</sup> Os (ppt)	±	<sup>187</sup> Re/ <sup>188</sup> Os	±	<sup>187</sup> Os/ <sup>188</sup> Os	±	rho	% Re Blank	% <sup>187</sup> Os Blank	% <sup>188</sup> Os Blank	Os <sub>i</sub> @ 130 myr*	Os <sub>i</sub> @ 125 myr*	Os <sub>i</sub> @ 124 myr*	Os <sub>i</sub> @ 123 myr*	±
TM01	Black Shale	24.5	15.5	64565.7	2.5	689.0	2.2	0.006	69.4	0.4	22.2	0.1	197.2	1.2	2.362	0.019	0.654	0.68	0.01	0.15	1.93	1.95	1.96	1.96	0.02
TM02	Mudstone	24.6	12.3	58397.8	1.6	819.9	1.3	0.004	73.3	0.6	23.9	0.2	108.4	1.0	2.181	0.027	0.677	1.00	0.02	0.17	1.95	1.96	1.96	1.96	0.03
TM03	Black Shale interbedded Marl	43.1	17.9	11182.5	219.9	13741.5	33.7	0.082	273.5	1.6	76.6	0.3	875.6	4.0	3.757	0.020	0.606	0.08	0.01	0.10	1.86	1.93	1.95	1.96	0.03
TM04	Black Shale interbedded Marl	42.1	13.0	6245.9	309.8	22864.5	26.5	0.065	248.2	1.4	71.2	0.3	741.2	3.4	3.489	0.019	0.609	0.10	0.01	0.11	1.88	1.94	1.96	1.97	0.02
TM05	Black Shale interbedded Marl	44.2	18.3	8424.5	180.8	16525.3	20.9	0.051	237.2	1.4	69.4	0.3	598.4	2.7	3.276	0.018	0.610	0.12	0.01	0.12	1.98	2.03	2.04	2.05	0.02
TM06	Black Shale interbedded Marl	45.8	15.5	4802.9	378.3	28062.1	24.9	0.062	234.9	1.4	67.2	0.3	737.4	3.4	3.522	0.019	0.609	0.10	0.01	0.12	1.92	1.99	2.00	2.01	0.02
TM07	Mudstone	37.5	5.1	17730.9	3.1	9703.3	0.7	0.003	26.8	0.2	8.6	0.1	174.0	1.8	2.333	0.031	0.704	1.73	0.05	0.47	1.96	1.97	1.97	1.98	0.03
TM08	Mudstone	34.5	6.1	23893.2	3.1	835.0	1.0	0.003	31.3	0.3	10.0	0.1	204.4	2.1	2.405	0.031	0.697	1.27	0.04	0.40	1.96	1.98	1.98	1.99	0.03
TM09	Mudstone	23.8	12.6	64566.5	0.7	440.5	0.6	0.002	42.4	0.3	14.2	0.1	85.5	0.9	1.922	0.024	0.657	2.13	0.04	0.28	1.74	1.74	1.75	1.75	0.03

<sup>^</sup>Total Os abundance.

<sup>#</sup>EF is the Enrichment Factor where EF<sub>element</sub> X = (X ÷ Al sample) ÷ (X ÷ Al upper crust) (Algeo and Maynard, 2004; Tribovillard et al., 2006).

\*Os<sub>i</sub> = the calculated initial <sup>187</sup>Os/<sup>188</sup>Os composition at a given depositional age.

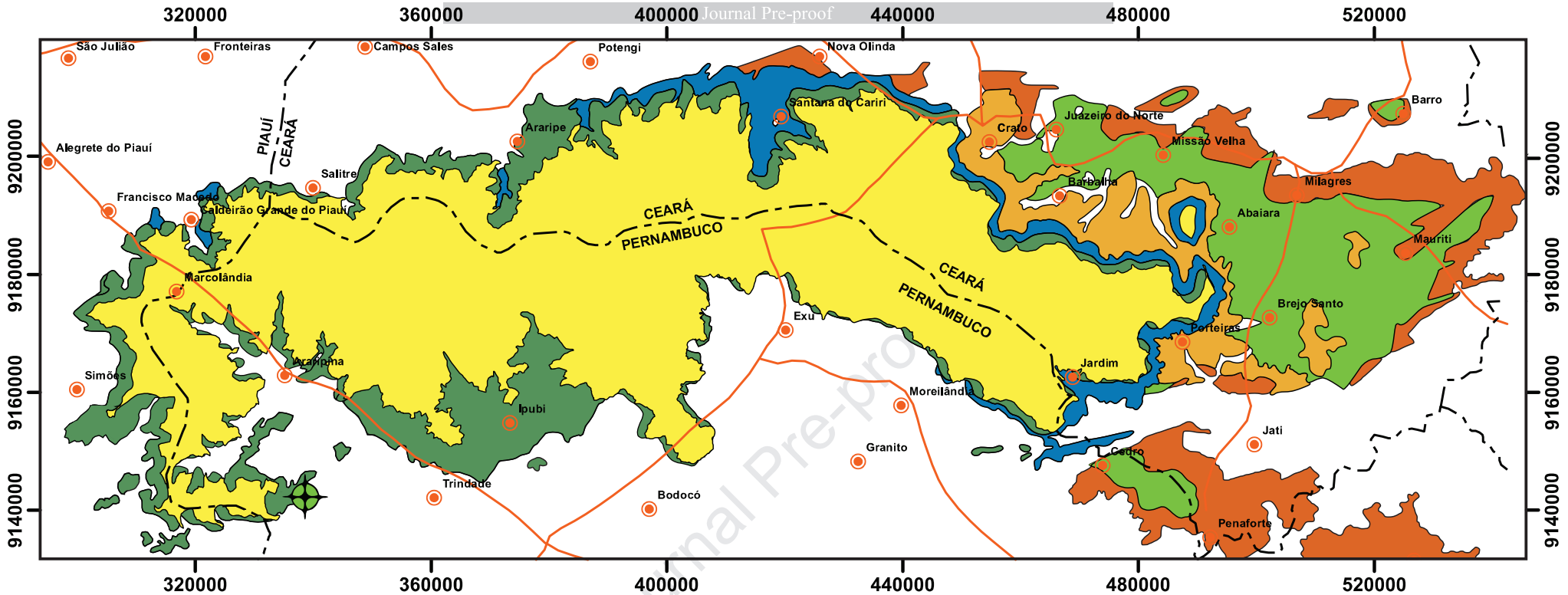




## BORBOREMA PROVINCE

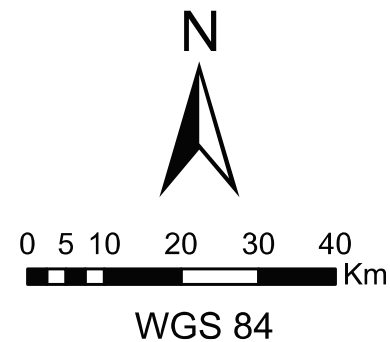
- Araripe Basin
- Sedimentary Basin
- Paleoproterozoic Granitoid
- Neoproterozoic Granitoid
- Médio Coreaú Domain
- Cearence Domain
- Rio Grande do Norte Domain
- Transversal Zone Domain
- South Domain



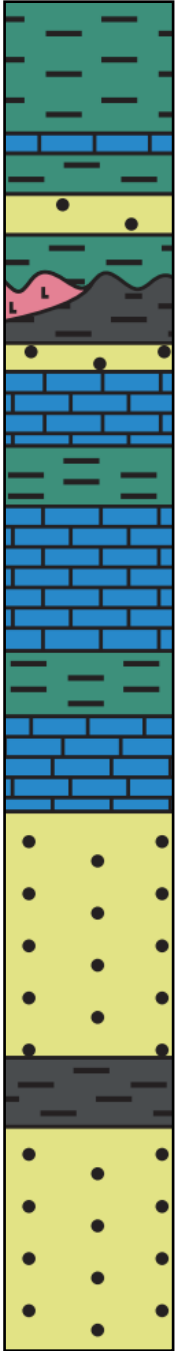


LITHOSTRATIGRAPHIC UNITS		TECTONIC SEQUENCE
Araípe Group	Exu Fm.	Post-Rift II
	Araípe Fm.	
Santana Group	Romualdo Fm.	Post-Rift I
	Ipubi Fm.	
	Crato Fm.	
Vale do Cariri Group	Barbalha Fm.	Rift
	Abaíara Fm.	
	Missão Velha Fm.	
Vale do Cariri Group	Brejo Santo Fm.	Pre-Rift
	Cariri Fm.	
Basement		Intracratonic

- Sampling Location
- City
- States Boundary
- Highway



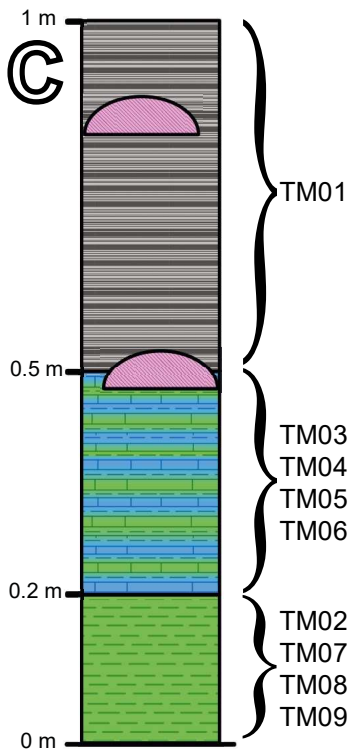
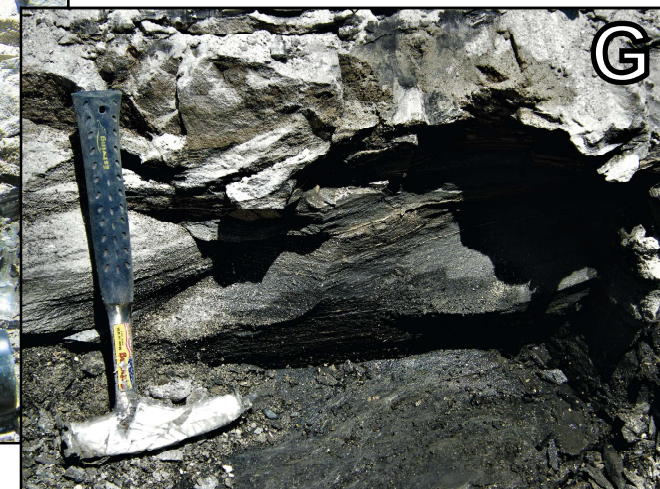
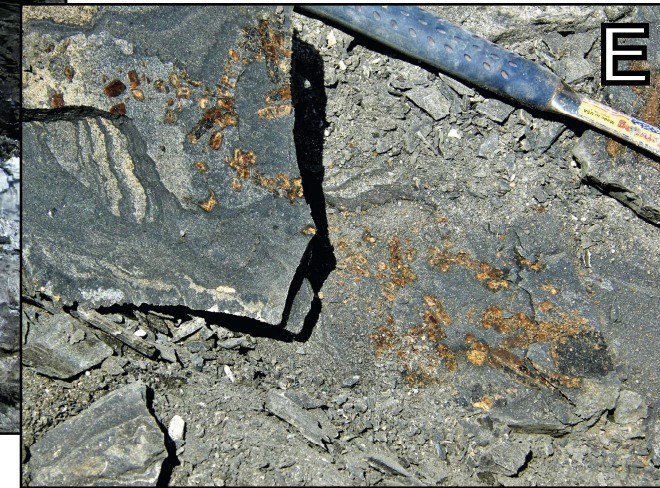
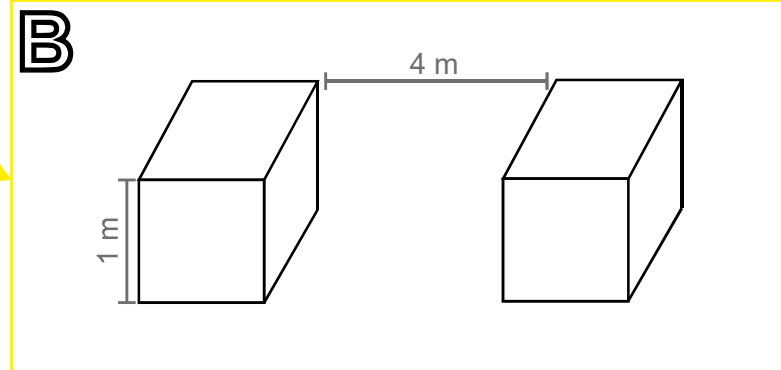
Romualdo Formation
Ipubi Formation
Crato Formation
Barbalha Formation







Coimbra et al. (2002)		Tomé et al. (2014)	
Biozones	Chronostratigraphy	Biozones	Chronostratigraphy
<i>Cytheridea</i> spp.	Aptian-Albian	<i>Pattersonocypris angulata</i>	Aptian-Early Albian
<i>Cicatricosisporites avnimelechi</i>		<i>Pattersonocypris micropapillosa</i>	
<i>Cytheridea</i> spp.		<i>Darwinula leguminella</i>	
<i>Cytheridea</i> spp.		<i>Cypridea araripensis</i>	
<i>Cicatricosisporites avnimelechi</i>	Late Aptian	<i>Neuquenocypris (Protoneuquenocypris) antiqua</i>	
<i>Sergipae veriverrucata</i>		<i>Rhinocypris scabra</i> <i>Damonella ultima</i>	
<i>Cytheridea</i> spp.	Aptian-Albian		
<i>Sergipae veriverrucata</i>	Late Aptian		

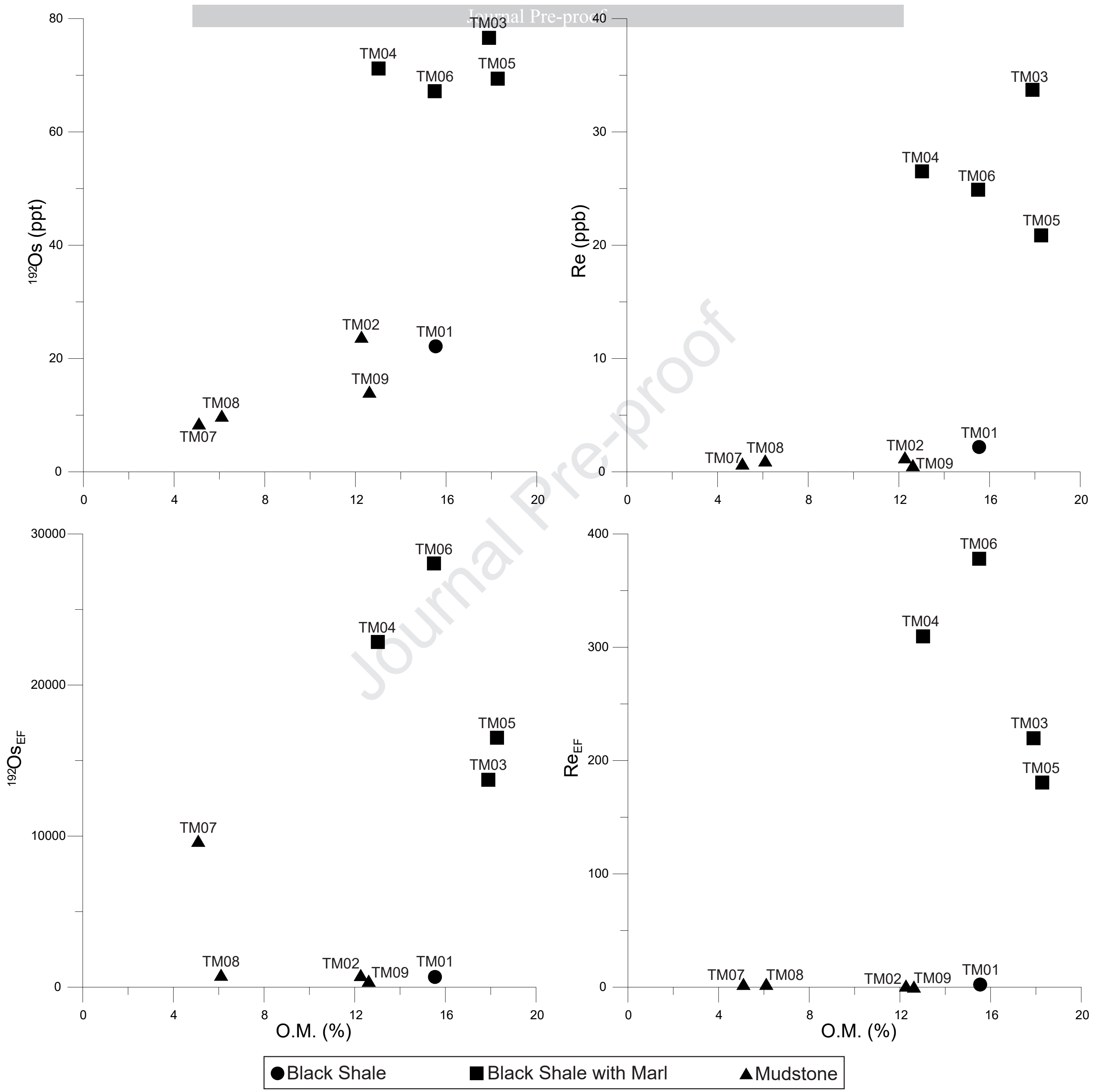
- Evaporite
- Black Shale
- Sandstone
- Shale
- Limestone

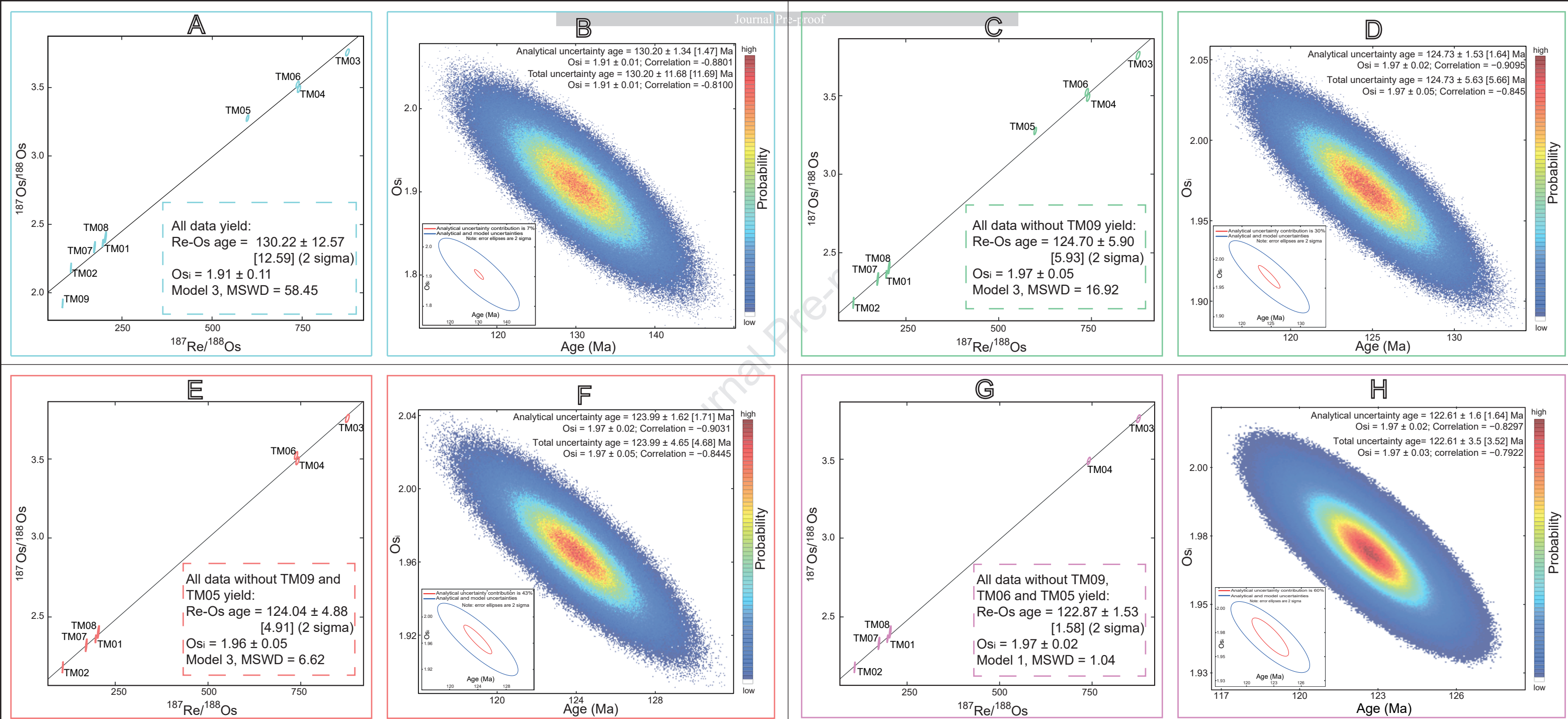




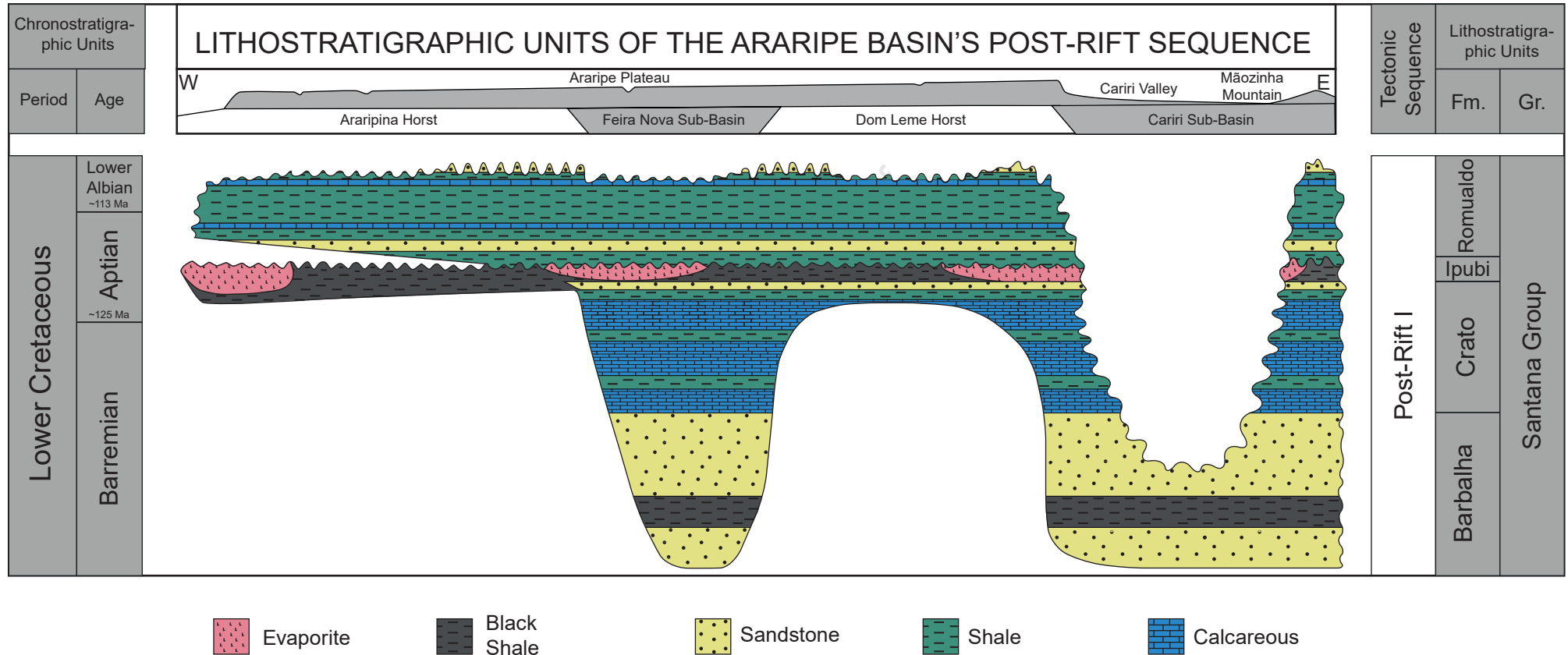
-  Black Shale
-  Black Shale interbedded Marl
-  Gypsum Lense
-  Mudstone













The Highlights considered for the manuscript are:

1. The first Re-Os absolute age ( $123 \pm 3.5$  Ma) for Ipubi Formation black shales in the Araripe Basin indicates the formation is Late Barremian / Early Aptian and not Aptian / Albian, and was deposited prior to the onset of OAE1a.
2. Based on the Re-Os age a new chronostratigraphic model is proposed for the Santana Group, Araripe Basin.
3. Highly radiogenic  $^{187}\text{Os}/^{188}\text{Os}$  compositions of  $1.97 \pm 0.02$  imply that the Araripe Basin records a highly restricted water mass during the Late Barremian / Early Aptian.

## **AUTHORS CONTRIBUTIONS**

*THALES LÚCIO*: Conceptualization; Validation; Formal analysis; Resources; Writing - Original Draft; Writing - Review & Editing; Visualization.

*JOÃO ADAUTO SOUZA NETO*: Conceptualization; Validation; Writing - Review & Editing; Project administration; Funding acquisition.

*DAVID SELBY*: Conceptualization; Methodology; Validation; Formal analysis; Investigation; Resources; Data Curation; Writing - Original Draft; Writing - Review & Editing; Supervision; Project administration.

**Conflict of Interest**

February 18, 2020

Editorial Department of Journal of South American Earth Sciences

Dear Editor-in-Chief,

We strongly request that the manuscript is not reviewed by any member of the AIRIE research group led by Holly Stein at Colorado State University because of the previous publication history and importantly at present Holly Stein and co-workers are working in the same competitive area, and there is a potential for conflict of interest.

Thank you for your consideration and we look forward to hearing from you.

Sincerely,

Thales Lúcio, PhD Student

Geochemistry Laboratory Applied to Petroleum  
Department of Geology  
Graduate Program in Geosciences, Federal University of Pernambuco  
Avenida da Arquitetura, s/n, Cidade Universitária  
Recife, Pernambuco, CEP: 50.740-550, Brazil  
Tel.: +55-81-21268240; Fax: +55-81-21268234; e-mail: thaales.lucio@gmail.com